

UNLIMITED
DISTRIBUTION
ILLIMITÉE

**Communications
Research
Centre**

**AN F-LAYER MODEL OF THE
IONOSPHERE FOR NORTH AMERICA**

by

C.J. Gladwin

This work was sponsored by the Department of National Defence, Research and Development Branch
under Project No. 33G01

DEPARTMENT OF COMMUNICATIONS
MINISTÈRE DES COMMUNICATIONS

CRC REPORT NO. 1337

TK
5102.5
C673e
#1337

IC

CANADA

OTTAWA, SEPTEMBER 1980

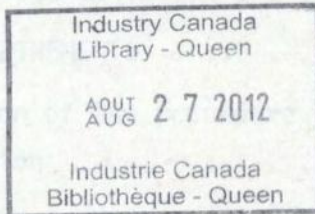
COMMUNICATIONS RESEARCH CENTRE

DEPARTMENT OF COMMUNICATIONS
CANADA

AN F-LAYER MODEL OF THE IONOSPHERE FOR NORTH AMERICA

by
C.J. Gladwin

(Radar and Communications Technology Branch)



CRC REPORT NO. 1337

September 1980

OTTAWA

This work was sponsored by the Department of National Defence, Research and Development Branch under Project No. 33G01

CAUTION

The use of this information is permitted subject to recognition of
proprietary and patent rights.

TK
SLO2.5
C6730
#1337
c.b

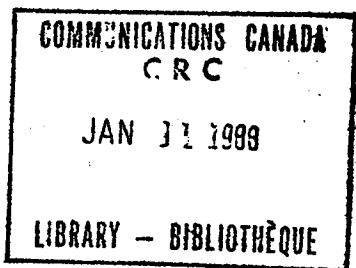


TABLE OF CONTENTS

ABSTRACT 1

1. INTRODUCTION 1

2. ALOSYN MODEL 5

 2.1 Description of the Data Base 5

 2.2 Development of the Model 9

 2.2.1 Organization of the Data Base 9

 2.2.2 Geographic Smoothing and Interpolation 10

 2.2.3 Sunspot Standardization 15

 2.3 Implementation of the Model 24

 2.3.1 Real Time Accession of the Data 24

 2.3.2 Correction to the User's Rz and Kp 24

 2.3.3 Interpolation to Month and Local Time 26

 2.3.4 Illustration 27

3. N(h) MODEL 34

 3.1 Description of the Data Base 34

 3.2 Development of the Model 35

 3.2.1 Organization of the Data Base 35

 3.2.2 Definition of the Profile Using ALOUETTE NH 37

 3.2.3 Definition of Profile Using Ground Echoes 42

 3.2.4 Illustration 44

4. MAIN TROUGH REFINEMENTS 52

 4.1 Description of the Procedure 52

 4.2 Illustration 53

5. ACKNOWLEDGEMENT 57

6. REFERENCES 58

7. BIBLIOGRAPHY 60

APPENDIX A - Glossary of Files and Tapes 65

APPENDIX B - List of Notations 77

AN F-LAYER MODEL OF THE IONOSPHERE FOR NORTH AMERICA

by

C.J. Gladwin

ABSTRACT

Data collected from the Alouette 1 and 2 satellites (ALOSYN and ALOUETTE N(h)) have been organized in order to make predictions of ionospheric characteristics such as foF2, slab thickness, and spread F as functions of longitude, latitude, local time, month, magnetic activity, and sunspot number. Spread F and foF2 are determined statistically from about 10^6 Alouette 1 ionograms and slab thickness is estimated using about 10^5 electron density profiles. The data and the necessary computer programs for analysing these data by the user are on two labelled tapes and are available from the Communications Research Centre. Contour maps of foF2, spread F and slab thickness as a function of geographic latitude and local time can be generated. A special technique is outlined in order that the user may modify his results to include the main trough. The major computer programs used are available on request.

1. INTRODUCTION

The Alouette 1 Topside Sounder satellite was launched on September 29, 1962. From that date until end of 1968, a continuing effort of the Defence Research Board Telecommunications Establishment (DRTE, the forerunner of the Communications Research Centre, CRC) was to routinely scale the approximately 1,000,000 ionograms recorded, for several ionospheric characteristics such as the F2 layer penetration frequency, foF2, as well as a subjective spread index in the neighbourhood of that point. The data have been stored on magnetic tapes and have come to be known as ALOUETTE 1 IONOSPHERIC DATA, ALOSYN [1].

Concurrently, 60,000 of these ionograms as well as another 20,000 Alouette 2 ionograms were scaled for "almost-complete" topside electron density profiles (that is within about 3% of the foF2). These data likewise have been stored on magnetic tapes and become known as ALOUETTE 1 (or 2) IONOSPHERIC DATA, N(h) [2].

The intent of this report is to describe a procedure for organizing and reducing these vast quantities of data in order that a user can obtain predictions of various ionospheric characteristics (foF2, spread, slab thickness, and possibly MUF(3000)F2) as functions of longitude, latitude, local time, sunspot number, month, and magnetic activity (as measured by the 3-hourly Kp index). It should be noted that while MUF(3000)F2 was not a scaled parameter, it can be computed from an estimated height of the maximum electron density by means of an empirical formula given by Shimazaki [27] or Schmid et al [26]. In addition to the prediction of various characteristics, the model has the capabilities of computing percentiles for the characteristics. A technique is also presented to enable the user to estimate regions of severe density gradients such as the main trough [17]. It is intended that the model also be used to supplement the work of Muldrew and James [19] in which the ionospheric effect on the Doppler frequency of a Search and Rescue satellite was estimated.

Global ionospheric modelling using vast quantities of data came of age in the early 1960's with the advent of easy accessibility to large computers. The first major one was the C.C.I.R. model which is accessible either through an atlas of ionospheric characteristics [5] or a companion punched card version. On a smaller scale (geographic latitude > 35°N), there exists the Canadian model [23] and that of Petrie [20]. Essentially these models are based on monthly medians of scaled characteristics for each hour of local time; the latter being observed at about 100 ground stations around the globe. The time frame was the five years in the mid 1950's corresponding to the rising part of the sunspot cycle. Using the numerical mapping procedures developed by Jones and Gallet [13], these data were reduced to sets of monthly coefficients for each characteristic, and then these sets were normalized to two sunspot numbers (Rz=0 and Rz=100). The predictions were assumed to vary linearly with sunspot number for Rz in [0, 150] and be independent of it otherwise.

The next extensive modelling exercise was culminated by Llewellyn and Bent [15]. Again they predicted foF2 from a set of bottomside stations (400,000 ionograms), but in addition they used the 60,000 Alouette 1 profiles and 6,000 electron density probe results (1967-68) to construct a "closed form" density profile. The inputs for their model were longitude, latitude, time, season, solar flux, sunspot number, and foF2. Their closed form profile essentially ignored underlying layers and ledges (F1, E, and D) because they were primarily interested in obtaining accurate values for total electron content, TEC, only. Thus their bottomside TEC could be used in conjunction with the present model, in place of the approximation to be outlined later.

For discussion and listings of some other modelling experiences one should see Kohnlein [14]. Another model, which will be applied here, is one of the trough created by Halcrow and Nisbet [10].

The model to be outlined in this report will now be considered. While there are 1,000,000 topside ionograms the vast majority of these is limited to the continents of North and South America; see Figure 1. However, unlike the data base for the bottomside models, there exists virtually continuous latitudinal coverage. Due to the precession of the orbital plane of Alouette 1 and the revolution of the earth about the sun, observations at a given latitude are obtained for two 4 hour local time intervals per month. The local time history of Alouette 1, coincidentally, repeats itself almost exactly every six months. Hence, the local time is essentially the same at a given geographic latitude for a given day of any year. Thus, in making predictions for a given month, at least 3 months of data will be required. On the other hand instead of using monthly medians of characteristics, semi-monthly medians will be used because of the nature of the local time cells. A few other minor nuisances, arising essentially from attempting to design an empirical model after the data have been collected, are also noted:

- (1) Because the satellite's solar cells degraded, the number of observations for the last 3 years of the recording process was virtually halved (see Table 2). Thus, there will be a "bias" in the model towards the lower sunspot years 1963-66.

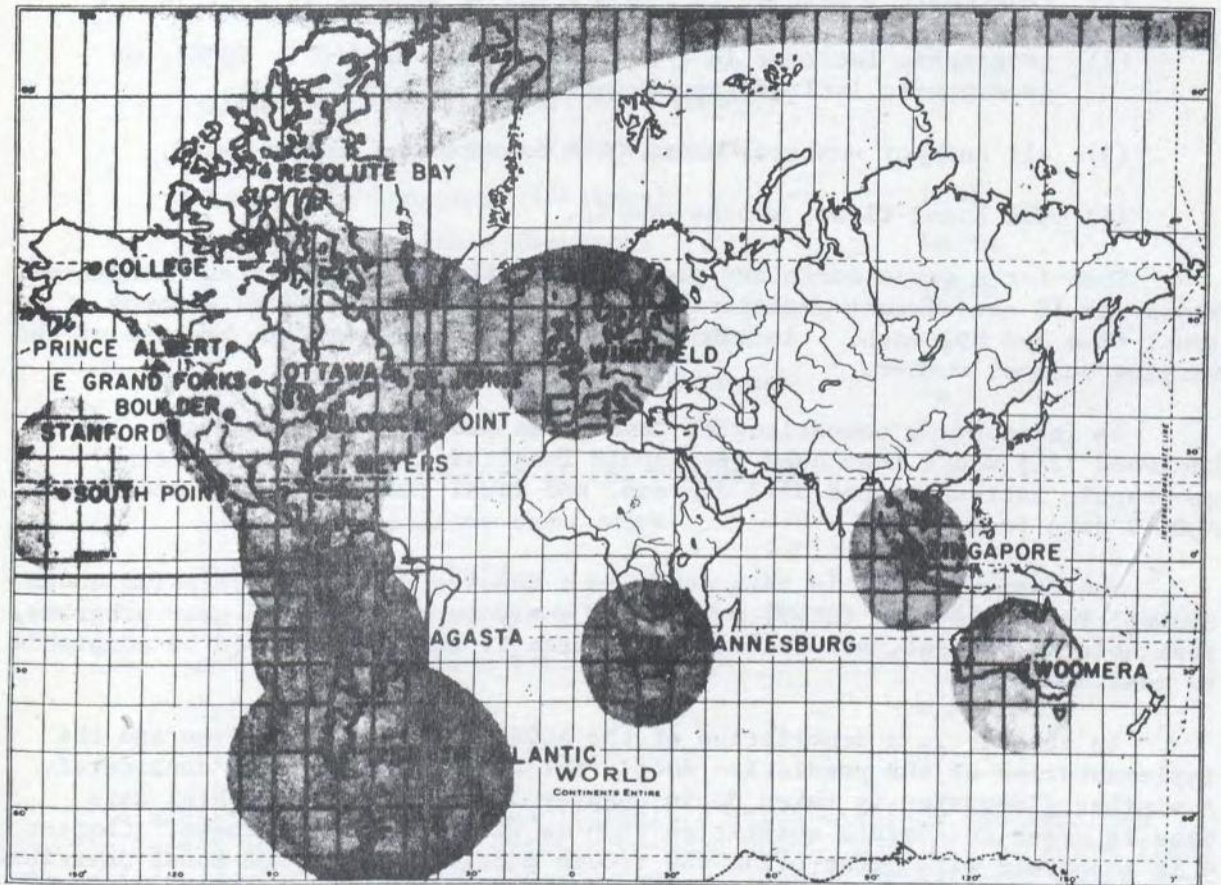


Figure 1. Location and Coverage of Alouette 1 Telemetry Stations. After [3]

- (2) Because of the routine scaling procedures, and possible change in habits of the scalars over the 6 year period, the number of observations (of foF2 or fxf2) which are "unreliable" (i.e. scaled to an uncertainty of more than 0.2 MHz) can range up to 60% in any given month (see Table 2). This problem of routine scaling is not as serious for the N(h) data, however, as these ionograms were scaled on user demand.
- (3) No data are available over the geographic poles (due to the 80° inclination of the orbital plane of Alouette 1).
- (4) The spread index may not be as consistent as that obtained in smaller scale spread experiments [4].
- (5) The maximum sounding frequency of Alouette 1 is 11.5 MHz. Hence, this model cannot give accurate foF2 values if the expected value exceeds about 10 MHz. The model will often give foF2 values greater than 11.5 MHz due to extrapolation to high sunspot numbers.

Only a model for North America, where most of the data were measured, is considered (see Figure 1). The actual domain for the model will be:

- (1) geographic longitude in $[-180^\circ, -45^\circ]$, that is $[180^\circ\text{W}, 45^\circ\text{W}]$,
- (2) geographic latitude in $[-10^\circ, 80^\circ]$, that is $[10^\circ\text{S}, 80^\circ\text{N}]$, or geomagnetic latitude approximately in $[0^\circ, 90^\circ]$,
- (3) all sunspot numbers, using CCIR assumptions for $R_z > 150$,
- (4) all local times, months and K_p .

Then for a given month and year, there will be 3 equidistant longitude zones and 18 equidistant geomagnetic latitude zones, as well as 4 zones of local time and K_p , each. Initially the year is kept separate because of the varying sunspot number.

An interesting comparison of results is provided by Petrie and Lockwood [21] where they used geographic longitude zones of 30 degrees, geographic latitude zones of 2 degrees, and local time zones of 1 hour for ALOSYN data from 1963.

The computer used in this study is a Honeywell Sigma 9 operating under Control Program - Five (CP-V). The data analysis programs and user programs, available on request, are written in Fortran IV and hence should be adaptable to most computers.

In chapter 2, a description of the ALOSYN data base is given and the implementation of the prediction model, for foF2 and spread, is considered. A similar discussion is taken up in chapter 3 for the ALOUETTE N(h) data base in order to compute quantities such as TEC and slab thickness. Chapter 4 is concerned with integrating the trough model [10] with the model described here. The notations used are summarized in Appendix B. A glossary of files and tapes is given in Appendix A relating the various programs to their respective sections in the report. A brief description of the files referred

to in the text is also given in Appendix A. A source listing of the files is also available on request.

2. ALOSYN MODEL

2.1 DESCRIPTION OF THE DATA BASE

The entire collection of 1,000,000 ionograms is stored on 8 9T (9 track) tapes in year-universal time order. They have been blocked into 3200 byte records. Each record contains at most 40 ionograms with 80 bytes of information. A new record is started with each day change. There is an 80 byte header, or title, to be skipped at the beginning of each tape. A header has also been placed at the beginning of some months. A complete description of all the data in a record may be found in Nelms et al. [3] or at the beginning of any of the monthly or semi-monthly ALOSYN booklets [1] that have been published. Here only a list of the data actually used in the model is presented:

Year	Y
Month	M
Day	D
Universal time (hour, minute, second)	Ut
Geographic local time (hour, minute)	Lt
Geographic longitude (degrees)	Long
Geographic latitude (degrees)	Lattg
Geomagnetic latitude (degrees)	Lattm
Height of the satellite (kilometres)	h_s
Solar angle at the satellite (degrees)	χ_s
Gyrofrequency at the satellite (MHz)	$f_H(h_s)$
Penetration frequency of the O wave (MHz)	foF2
Accuracy of scaling the O wave	a(o)
Spread of the O wave	s(o)
Penetration frequency of the X wave (MHz)	fxF2
Accuracy of scaling the X wave	a(x)
Spread of the X wave	s(x)
Planetary magnetic activity index	Kp

In addition, one should consult Table 3 which displays the smoothed monthly Zurich sunspot numbers which have been used. Most of the above items are self-explanatory; also see the accuracy and spread definitions which may be found in Tables 1(a) and 1(b) respectively.

TABLE 1(a)
Accuracy Convention of ALOSYN foF2

a (o)	Definition
1	foF2 within .05 MHz of tabulated value
2	foF2 within .1 MHz of tabulated value
3	foF2 within .2 MHz of tabulated value
4	foF2 less than tabulated value
5	foF2 greater than tabulated value
-0	foF2 not observed

TABLE 1(b)
Spread Convention of ALOSYN

s (o)	Definition	Index
A, B, C	No spread	1
D, E, F	Slightly spread	2
G, H, I	Moderately spread	3
J, K, L	Extremely spread	4

In Table 1(a) there is some doubt about the interpretation of a=4 or 5, due to changes in scaling habits over the years. In the early years these appear to have meant an uncertainty greater than 0.2 MHz and a -0 was used for "unobservable" critical frequencies. However, the correspondence given in the table, a in [1,5], is adopted for all years. Using this table, foF2 is defined for each ionogram, as follows (see Appendix B).

$$f_{oF2} = \begin{cases} [f_{xF2}(f_{xF2} - f_H(h_{max}))]^{1/2}, & \text{for } a(x) \text{ in } [1,3] \\ f_{oF2}, & \text{for } (a(o), a(x)) \text{ in } [1,3] \times [4,5] \end{cases} \quad (2.1)$$

where $f_H(h_{max})$ is found by an inverse cube extrapolation from h_s to $h_{max} = 300$ km.

In Table 1(b) the three letters associated with each group were used to record other information (e.g. oblique traces, cusps, etc.), but the index at the right will be sufficient here. In a similar vein, Kp values defined as n-, no, or n+ are taken to be $n - .3$, n, or $n + .3$ where n is an integer in [0,9].

TABLE 2
Blocked ALOSYN Records and Percentage of Unreliable Ionograms by Month and Year

YEAR MONTH	1962	1963	1964	1965	1966	1967	1968
JANUARY	-	507 10	485 28	458 45	228 42	235 29	136 44
FEBRUARY	-	495 21	439 26	412 52	301 56	230 26	166 42
MARCH	-	503 28	428 25	463 48	198 30	268 26	171 41
APRIL	-	562 19	554 18	571 38	302 18	285 20	213 26
MAY	-	621 13	577 15	600 18	334 18	269 20	214 34
JUNE	-	493 6	418 21	502 21	328 18	285 21	215 34
JULY	-	592 10	582 13	610 18	261 12	271 18	228 22
AUGUST	-	615 11	495 26	590 23	180 24	266 19	203 32
SEPTEMBER	20 16	465 15	392 31	433 24	230 22	256 24	172 31
OCTOBER	613 34	602 28	316 32	561 28	258 20	274 25	164 38
NOVEMBER	637 29	599 26	519 49	406 38	190 32	199 37	170 49
DECEMBER	506 28	479 26	419 62	271 46	173 27	143 50	137 51

TABLE 3
Zurich (Smoothed) Sunspot Numbers, Rz

YEAR MONTH	1962	1963	1964	1965	1966	1967	1968	1969	1970	1971	1972
JANUARY	41.5	28.9	18.2	12.1	28.8	72.3	100.4	110.5	103.1	76.7	71.3
FEBRUARY	38.9	29.9	16.2	12.1	32.2	75.7	101.3	109.2	104.2	74.1	71.7
MARCH	37.9	29.0	13.1	13.1	35.0	78.9	103.8	106.7	105.0	70.5	72.8
APRIL	38.2	28.7	10.6	15.1	37.8	81.1	106.7	104.3	105.6	66.9	73.6
MAY	37.6	28.5	9.4	15.3	41.8	83.9	107.5	106.5	105.5	64.3	72.8
JUNE	36.3	27.6	9.6	16.0	45.4	87.7	106.9	102.7	104.9	63.6	69.8
JULY	34.8	27.2	10.0	16.0	52.2	90.3	106.0	102.3	102.7	63.6	66.9
AUGUST	32.7	26.7	9.8	16.7	58.0	91.2	106.1	103.2	98.6	63.8	63.9
SEPTEMBER	30.6	26.5	9.5	17.8	65.0	91.2	108.6	101.9	94.4	65.8	60.3
OCTOBER	29.2	24.7	9.5	21.1	66.5	91.2	111.6	100.6	91.0	66.6	58.4
NOVEMBER	29.4	21.8	10.9	22.7	69.7	93.7	112.2	101.2	86.2	67.3	56.6
DECEMBER	29.0	19.5	11.4	25.2	71.0	97.8	111.3	101.9	80.4	69.9	53.2

In Table 2, the following statistics are displayed:

- (a) the actual number of (blocked) records with data, by month and year,
- (b) the percentage of "unreliable" ionograms, by month and year, i.e. those for which an foF2 is not definable, using equation (2.1). For example, for May 1965, there are 600 blocked records and 18% of the total number of ionograms are unreliable.

In view of the introductory remarks, the actual number of ionograms in a given month and year is approximately

$$I = 40 R - 20 D_m \quad (2.2)$$

where R = number of blocked records

D_m = number of days in month M

I = actual number of ionograms.

2.2 DEVELOPMENT OF THE MODEL

2.2.1 Organization of the Data Base

A description of how the data were processed is given here and in Figure 2. A description of how the user uses these processed data is given in section 2.3.

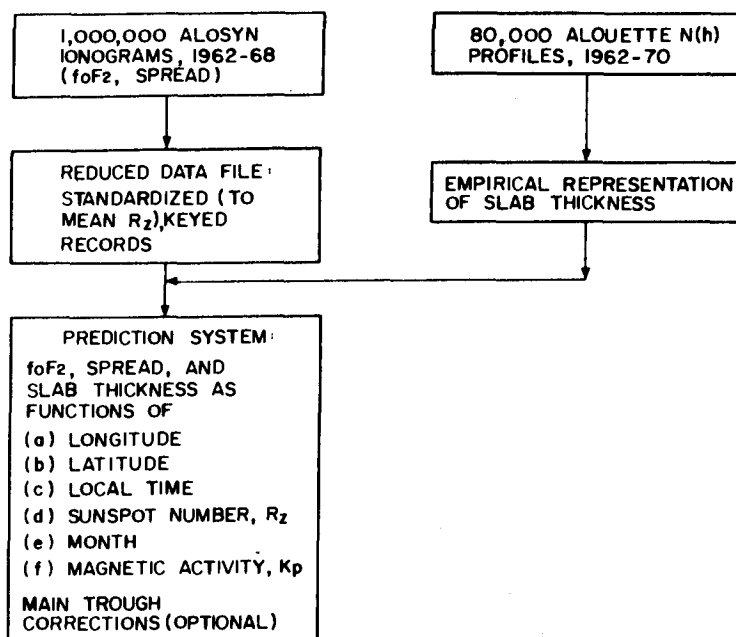


Figure 2. Schematic Overview of Model Development

Instead of processing the 8 tapes sequentially (i.e. year by year), they were processed month by month for all years. While this increases the requisite number of tape usages by (at most) a factor of $76/8 = 9.5$, it permits a modular processing procedure for the vast quantities of data (see below). Also, this procedure is more natural in the sense that convenient checks arise on the consistency of the data. Thus, the first step is to set up Nyear files for a given month, ALOMONXX, where Nyear is the number of years of data available for that month, and XX are the last two digits of the respective year represented by ALOMONXX. Each of these files contains $R + 1$ records (see Table 2), i.e. each file contains either the header for the month or the last record of the previous month, followed by the R records in the month. During this initial processing stage, in addition to completing Table 2, counts of the number of complete or partial records omitted due to "tape problems" are also kept. This is necessary in order to position the tape correctly, for starting the next month. Additional checks are provided by actually printing out the first 4 records as well as the last 3 of each of the files ALOMONXX. The control files AXX and BXX are then executed to continue the next stage of processing (see below).

2.2.2 Geographic Smoothing and Interpolation

In the first stage of this process, executing AXX, the ionograms are sorted into a number of longitudinal and latitudinal zones of essentially constant magnetic activity and local time. The longitude range is divided into 3 equal zones and the geomagnetic latitude range is divided into 18 equal zones (see the model domain given in chapter 1). Each of these 54 geographic areas (see Figure 3) is then subdivided into 4 magnetic activity zones defined by the ranges of Kp:

[0,1.3] ; [1.7,3.3] ; [3.7,5.3] ; [5.7,9.0];

and 4 local time zones (see below for a more complete description). Thus there are 864 cells, although many of these will be empty in the southwest corner (over oceans, see Figure 3, or Table 4). Furthermore the fourth Kp zone (corresponding to severe storms) is fairly scant in terms of data. However, the fine division is used to prevent features such as the main trough from becoming too "smoothed out"; the latter is strongly dependent on local time and Kp [17].

These zones define 864 cells. Associated with each of the 864 cells, a record is kept consisting of the following data array:

$(n_k, \text{Long}_k, \text{Lattm}_k, \chi_k, \text{Kp}_k, \text{Lt}_k, \text{foF2max}_k, \text{foF2min}_k)$ $k = 1(1)864,$

where n_k is the number of ionograms in the cell and the other numbers are arithmetical averages, minima or maxima of the respective observations in the cell. These data are placed on a scratch file DUMXX which is updated on the next pass through ALOMONXX by BXX. This update consists of appending a frequency distribution consisting of 10 equidistant intervals of $[\text{foF2min}_k, \text{foF2max}_k]$ for foF2, and also a distribution for the spread (with 4 intervals). The choice of 10 intervals for foF2 was partially motivated by the number of ionograms n_k being tabulated and also by the fact that the range $(= \text{foF2max}_k - \text{foF2min}_k)$ is roughly 2 MHz, so that the grouping process has an uncertainty

of about the same magnitude as the maximum scaling uncertainty (corresponding to accuracy $a = 3$).

This updated collection of 864 records is put on a file called MONXX together with the Long, Lattm, Lt, Kp, M, and Y subscripts (see below). This completes the first reduction which has seen an original ALOSYN month reduced by a factor of about 20 in computer storage. In the next section a further reduction by a factor of about 10 (by eliminating empty cells and standardizing to one sunspot number) will be carried out.

A brief description of the construction of the 4 local time zones and their respective indices is now given.

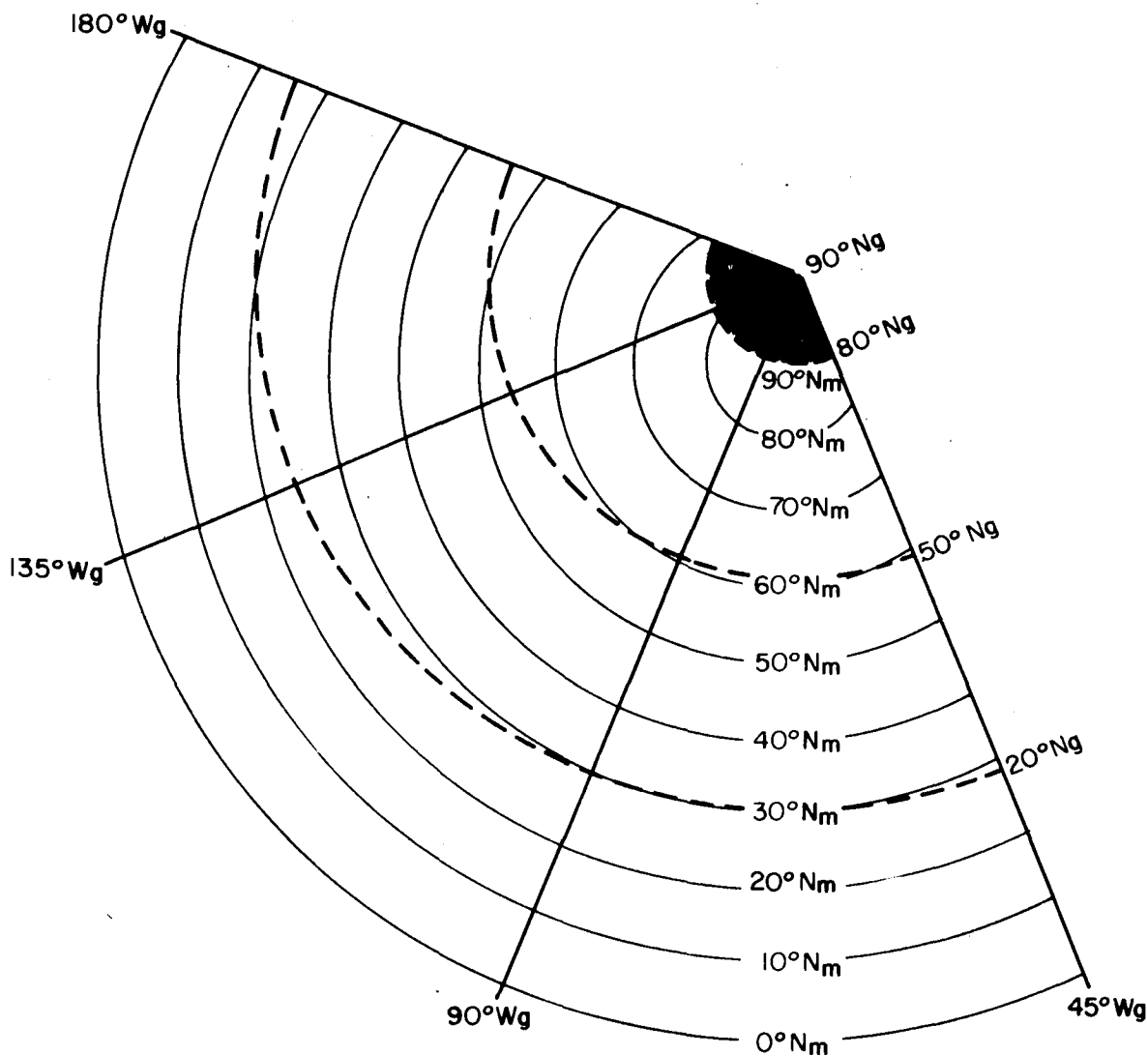


Figure 3. Geographic Zone Alignment of the ALOSYN Model

TABLE 4

*Number of Good Ionograms by Longitude and Latitude for February, all Years,
Local Times and Magnetic Activity.*

	GEOGRAPHIC LONGITUDE ($^{\circ}$ W)		
	[180,135)	[135,90)	[90,45]
[85,90]	-	306	3162
	-	2228	1759
[65,70]	1045	2328	1399
	1663	1387	1082
	1112	1268	1161
	884	1066	1108
	798	829	901
	693	681	826
	243	607	887
	41	461	791
	26	351	388
	74	183	316
[45,50]	68	47	283
	50	15	272
	32	13	244
	46	25	227
[20,25]	47	21	342
	10	16	455
[0,5)			

In Figure 4, three orbits of the satellite have been plotted (geographic latitude v. geographic local time) for the 1st, 16th and 31st of October. For other months, see the caption. The 4 zones are described by a pair of subscripts (LT1,LT2) defined on the product set [1,2] x [1,2], as shown in Figure 4. The first subscript defines the "half-month" that the particular ionogram is in and is determined by comparing the actual hour in the month (Greenwich) of the ionogram to the total number of hours in the month. The second subscript determines whether the ionogram is from a northbound (daytime, in this case) pass or not. This is determined by whether or not the local time of the ionogram is less than the theoretical local time at the maximum geographic latitude of the satellite (approximately 80°N), Ltmax. The latter has been computed assuming a linear variation with year fraction, Yf (where Yf, for example, for January 31 1963, is about 63.085).

$$Lt_{max} = 16.48 - 47.93(Yf - 62.74) \pm .05 \text{ hours, modulo } 24. \quad (2.3)$$

This empirical formula was determined by passing a straight line through the actual (Ltmax, Yf) pairs from 1962 day 272 at 2130 hours and 1966 day 274 at 0120 hours. At these times Alouette 1 was actually near 80°N and the actual values of Ltmax were computed by fitting a parabola to 5 (Lattg, Lt) pairs in the neighbourhood of 80°N.

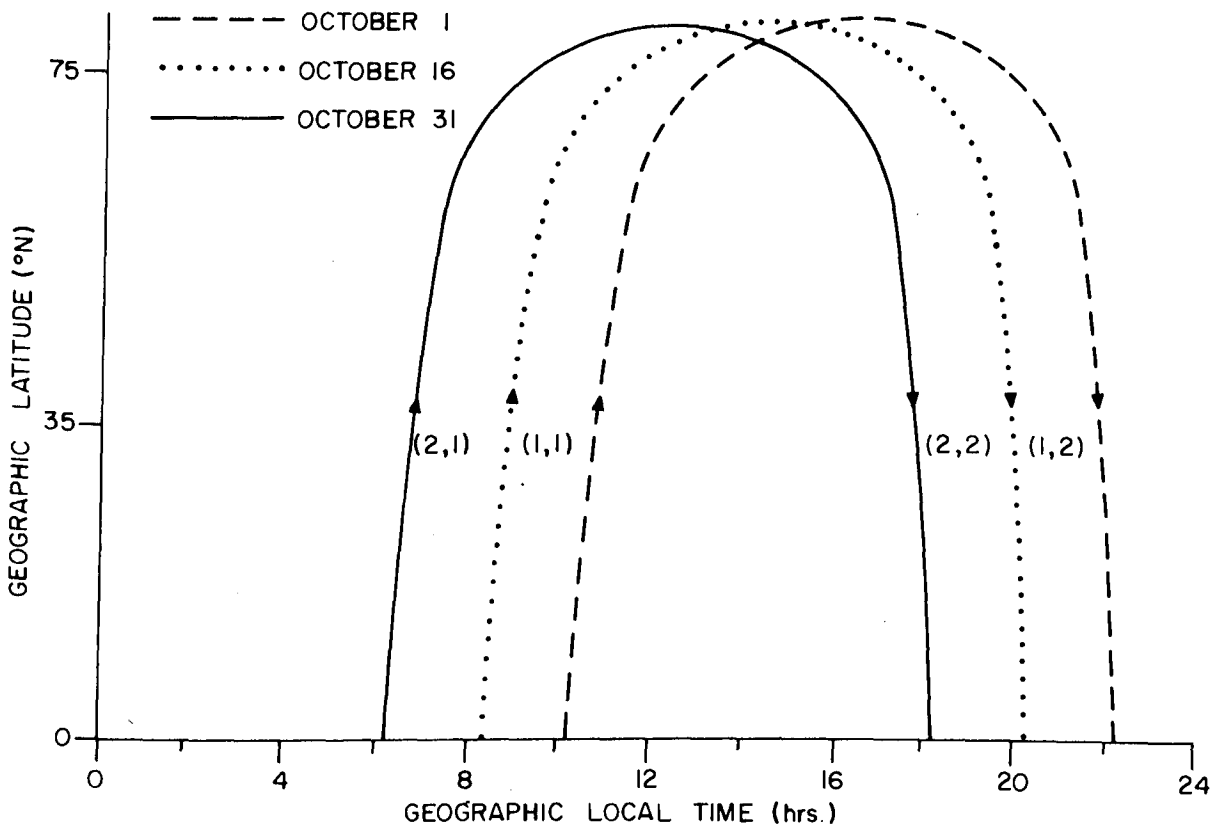


Figure 4. Definition of the Local Time Zones for October; April is the same. For November and May, December and June, January and July, February and August and March and September, Move the Curves 4,8,12,16,20 hours, respectively, to the Left.

Actually, the local time zones are not so symmetrically placed about Lt_{max} since geomagnetic latitude is used in defining the Lattm zones. Thus the 4 local time zones deviate from the expected 2 hour zone size (especially around the poles), but this was considered a reasonable "trade-off" in view of the well known alignment of foF2 contours with magnetic latitude (e.g. see [17]).

Finally, for calculating the average local time of cell k (to ensure continuity around midnight), the following recursive formula is used:

$$A_i = [(i-1) (A_{i-1} + 24r) + (Lt_i + 24s)] / i \quad (2.4a)$$

where $i = 1(1)n_k$, r and s are integers in [0,1] such that the quantity $|(A_{i-1} + 24r) - (Lt_i + 24s)|$ is a minimum. The average local time for cell k is

$$Lt_k = A_{n_k} \quad (2.4b)$$

A cell (or record) of any MONXX shall be referenced according to seven subscripts LO, LA, LT1, LT2, LK, LM, LY) defined on the (extended) product set

$$[1,3] \times [1,18] \times [1,2] \times [1,2] \times [1,4] \times [1,12] \times [2,8]$$

corresponding to the Long, Lattm, Lt (two values), Kp, M, and Y zones, respectively. The Long zones are numbered from west to east, the Lattm zones from north to south, the Lt zones as in Figure 4, the Kp zones with increasing magnetic activity, and the M zones from January to December. The Y zone is simply the second digit of "XX" in MONXX. After the standardization of the MONXX (see below), the year subscript, Y, will be dropped.

A single example of a record of MONXX is now given. A cell was chosen where the range of the foF2 distribution was considerably greater than 2 MHz, in order to illustrate the geographic smoothing involved in the model.

Example 1: Cell 1,5,2,1,3,2,7 ; February 1967.

The contents of the record are shown in Figure 5.

See also Example 2 to follow.

On actually examining the 7 ionograms which comprised the cell it was noticed that the 4 ionograms at the lower end of the foF2 range came from a locale (165°W, 68°N) at 1730 hours, while the upper 3 came a day later and an hour earlier at the locale (136°W, 66°N). Thus the two extreme points have been replaced by a hypothetical intermediate point, yielding a median foF2 of 4.5 MHz.

An extract from MONXX starting at cell (3,7,2,1,1,9,2) is shown in COMPUTER OUTPUT 1.

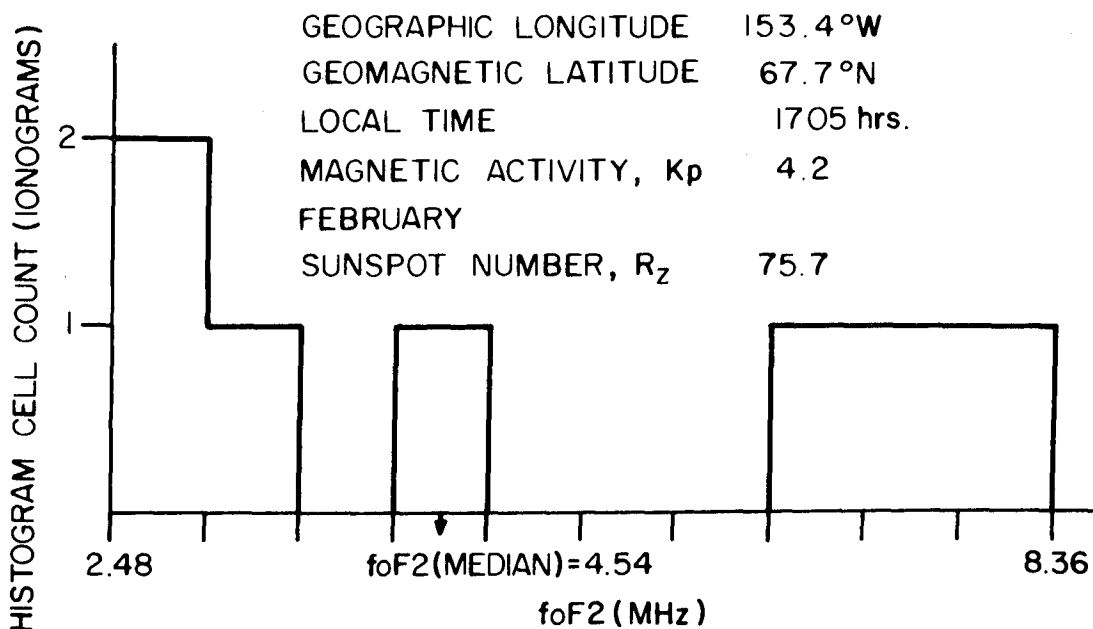


Figure 5. Distribution of foF2, for a Given Set of Conditions.

2.2.3 Sunspot Standardization

Here a procedure for reducing the Nyear files MONXX to a single file MON, of essentially the same form, but standardized to some central sunspot number depending on the respective sunspot numbers of the individual MONXX, will be described. The reason for selecting sunspot number (rather than any of the other 5 independent variables) is that ionospheric characteristics, e.g. foF2, have been observed to possess strong linear relationships with sunspot number, at least up to $R_z = 150$. See Davies [6], for example.

There are a number of ways in which this standardization procedure may be achieved; here the approach adopted in the C.C.I.R. model [5] is briefly described to note some of the difficulties in applying it to satellite observations. This provides some motivation for the procedure which was actually adopted.

For each of the 60 months (1954-58), the data for each hour of local time at approximately 100 ground stations have been used to determine a numerical map of the form:

$$foF2 = a_0 + \sum_{j=1}^6 a_{2j-1} \cos jT + a_{2j} \sin jT \quad (2.5)$$

where $T = 15 Lt - 180$ is the local time relative to noon, in degrees. Actually, each of the a_j are dependent on 76 coefficients to describe the longitudinal and latitudinal variations so that for each month (of 60) there are 988 ($= 76 \times 13$) coefficients in all. Then for a given month, (all years) and for each of the 988 coefficients, a least squares line is fitted to the coefficient versus sunspot number. From these relations, two sets of

988 coefficients are tabulated, for each month, corresponding to the sunspot numbers $R_z=0$ and $R_z=100$.

For a topside model, 72 months of data (1963-68) would have to be fitted to a map of the above form in 3 month stages at least (to ensure complete local time coverage). This would mean that the a_j would also have to depend on an extra variable, month, and perhaps even a K_p variable. This would give 24 (seasonal) sets of approximately 988 coefficients. Then for a given season and coefficient, a least squares line would be fitted to the coefficient versus "seasonal" sunspot number relationship. There can be quite a bit of variation of sunspot number with season -- especially during the years 1966-68 where the data are scantiest (see Table 2).

The procedure adopted here will be an "inverse" of the above - i.e. predictions are made for foF2 for a given set of conditions (Long, Lattm, Lt, K_p , and M from a given record of MONXX) and then these (at most) Nyear numbers (one from each year) are standardized to an intermediate sunspot number.

The Nyear files MONXX are first merged into one, MONB96, which has a blocked record format. That is, each record consists of the same cell for all years (864 blocked records). Unfortunately the number of ionograms varies considerably from year to year for a given cell. Probably an even more serious difficulty is that in trying to keep only "quality" cells (with Nyear or Nyear-1 years of data) the geographic coverage is drastically reduced overall. This is illustrated in Table 5 for 2 particular months.

For brevity, any such cell will be denoted as type (M,N). The M years are not necessarily the first M years (starting from 1962 or 1963), but in most cases this will probably be true. Thus, for example, if only cells with at least 2 years containing at least 2 ionograms are desired, the "practical minimum", only 447 cells out of 595 (75%) are kept for February.

The procedure actually adopted is to use only the (2,2) cells of MONB96. Thus for each of these cells a least squares fit is performed to the Nyear pairs of median foF2 and actual sunspot number to obtain:

$$\text{foF2} = a R_z + b \quad (2.6)$$

Then, in later interpolation and prediction (see section 2.3), only those cells which yield positive values of a and b are used. It is noted here that of the 10,368 (= 12 x 864) cells there are 5,618 of type (2,2). Of these, 586 gave non-positive values for a or b . Thus, for use in interpolation and prediction, (see section 2.3) there will be 5,032 (or approximately half of the total possible). As a matter of interest, it is noted that there are 1,005 cells (all months) which only contain 1 year of data. No attempt has been made to incorporate these cells into the model since coefficients a and b in (2.6) cannot be determined, independently, for each cell. Furthermore there are 126 cells (all months) which yielded values of $a > 0.1$. The majority of these are of "dubious" quality arising from calculating a and b with 2 or 3 years at essentially the same sunspot number.

While some of these coefficients (a and b) may be "rough", leading to "rough" values of foF2, these values will be smoothed out later (see section 2.3). This "roughness" and the effect of smoothing are illustrated in

TABLE 5

B(M,N). The Number of Blocked Records (Cells), for February and October, which have at Least *M* Years with at Least *N* Ionograms each Year.

FEBRUARY

$\begin{matrix} N \\ M \end{matrix}$	1	2	3	4	5	10	15	20
1	595	570	549	529	502	382	306	236
2	470	447	425	410	386	274	203	151
3	401	373	344	327	297	189	132	99
4	328	301	262	234	216	135	97	61
5	230	197	166	154	132	77	46	21
6	116	94	87	74	61	33	13	5

OCTOBER

$\begin{matrix} N \\ M \end{matrix}$	1	2	3	4	5	10	15	20
1	647	625	597	572	547	425	365	314
2	512	487	467	445	417	333	274	233
3	439	410	395	377	365	275	213	159
4	396	375	352	339	321	213	153	106
5	341	319	296	262	244	153	94	60
6	225	202	175	162	143	68	29	17
7	119	103	88	75	60	8	1	0

Figures 6(a) and 6(b). The local time of these plots is about 1730 hours at 45°N geomagnetic latitude. The actual regression model for the smoothed gradients, a (MHz/unit sunspot number), is:

$$\begin{aligned} a = & 0.053 - 0.011 \sin(\pi Lt/12) - 0.015 \cos(\pi Lt/12) \\ & + 0.016 \cos^2(\pi Lt/12) - 0.037 (Lattm/90) \\ & + 0.015 (Lattm/90)^4 - 0.046 (Kp/9.3)^3, \end{aligned} \quad (2.7)$$

with a root mean square error of ± 0.019 in a .

The equation (2.7) was determined by applying a stepwise regression procedure [24] to all February cells which yielded values of a and b . Only statistically significant (non-zero) coefficients (up to order 4) are displayed in (2.7).

The actual details of the standardization of a given cell of MONB96, assuming there are a "suitable" number of years containing a "suitable" number of ionograms are now given. One should also note Figure 7 where the mathematical assumptions underlying the standardization procedure are illustrated, namely:

- (1) the gradient of foF2 with sunspot number, a , is positive,
- (2) the intercept at $Rz = 0$, b , is positive,
- (3) the conditional probability distribution of foF2 for a given Rz is independent of Rz .

The following notations are used in the standardization procedure. Let $(n_k, Long_k, Lattm_k, Lt_k, Kp_k, Rz_k, Fmin_k, Fmax_k, (A_{ki} : i = 1(1)10, B_{ki} : i = 1(1)4))$ $k = 1(1) Nyear \geq 2$ denote a particular blocked record (cell) of MONB96. Here A_{ki} and B_{ki} are the histogram occurrence frequencies on $[Fmin_k, Fmax_k]$ and $[0.5, 4.5]$ for foF2 and spread, respectively. Note that

$$\sum_{i=1}^{10} A_{ki} = \sum_{i=1}^4 B_{ki} = n_k \geq 2$$

First the medians $M_k(F)$ and $M_k(S)$ are computed from the foF2 and spread histograms using inverse linear interpolation between the right-most abscissae and the cumulative histogram probabilities. Using the pairs $(Rz_k, M_k(F))$ $k = 1(1)Nyear$, regression coefficients a and b such that $foF2 = aRz + b$ are computed. Then using $Rz = \sum_{i=1}^{Nyear} Rz_k / Nyear$ the standardized limits of the foF2 histograms are computed:

$$SFmin = \min_k (Fmin_k + a(Rz - Rz_k))$$

and

$$SFmax = \max_k (Fmax_k + a(Rz - Rz_k))$$

The A_{ki} observations $F_{ki} = Fmin_k + (i - 0.5)h_k$ where $h_k = (Fmax_k - Fmin_k)/10$ are standardized to $SF_i = F_{ki} + a(Rz - Rz_k)$ and inserted into a histogram with

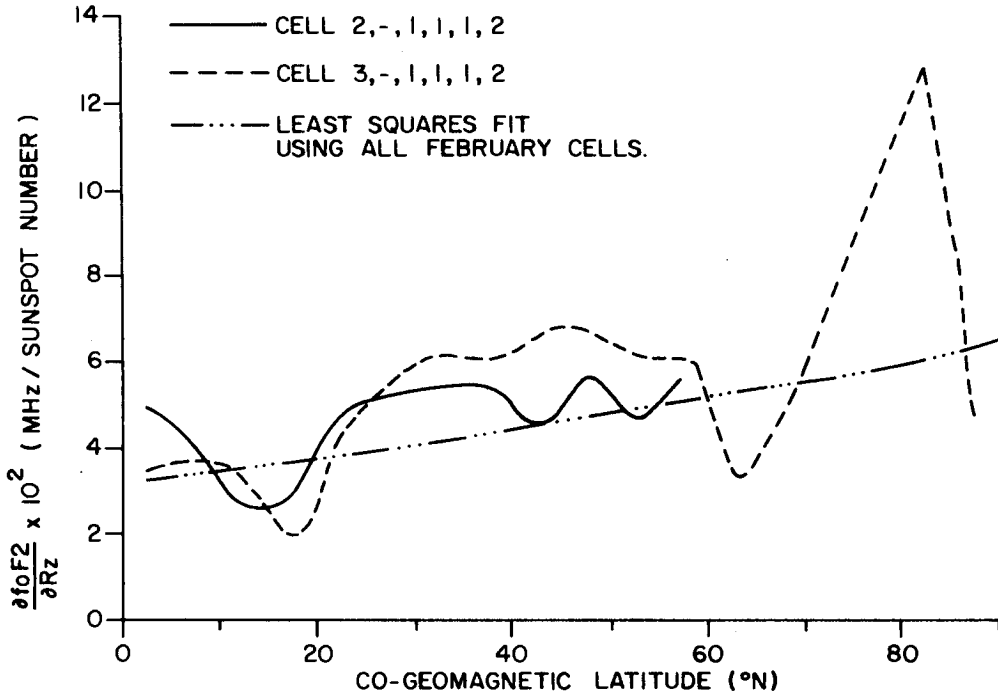


Figure 6(a). Behaviour of foF2-sunspot Number Gradient, $K_p < 1.5$.

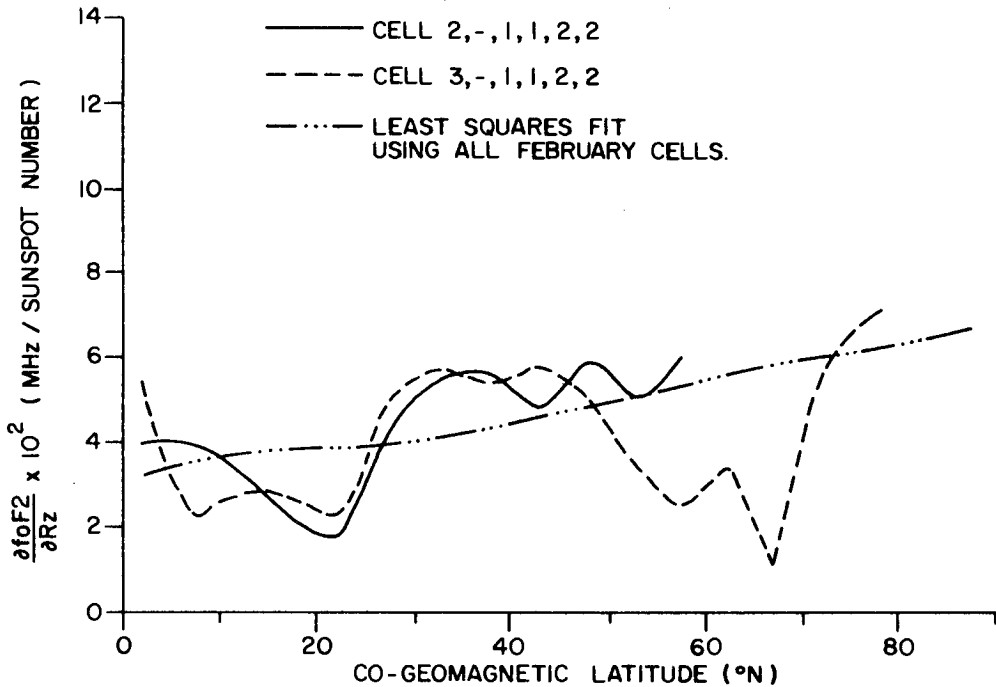


Figure 6(b). Behaviour of foF2-sunspot Number Gradient, $1.5 < K_p < 3.5$.

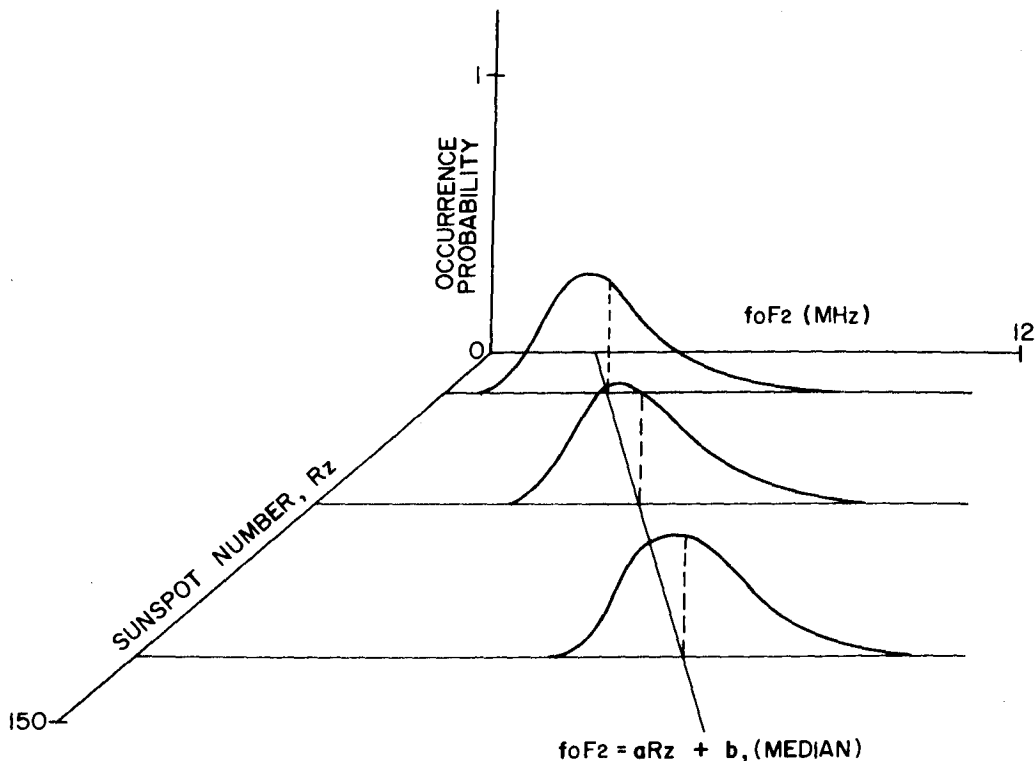


Figure 7. Assumptions Concerning the foF2 Distribution (for a Given Cell, all Years) Used in the Sunspot Standardization Procedure.

10 equidistant intervals on $[SF_{\min}, SF_{\max}]$ with occurrence frequencies SA_i .

Note that

$$\sum_{i=1}^{10} SA_i = \sum_{k=1}^{N_{\text{year}}} n_k = N.$$

In a similar fashion, one could standardize the spread distributions. However, due to the subjectiveness of that index they have been simply accumulated for all years. Essentially then, it is assumed that spread is independent of sunspot number. As a matter of interest, Figure 8(a) shows median spread plotted against sunspot number for 3 different cells. The local time of these cells is approximately 0900 hours in January and July and 1300 hours in December.

The spread occurrence frequencies are then:

$$SB_i = \sum_{k=1}^{N_{\text{year}}} B_{ki}, \quad i = 1(1)4$$

Finally arithmetical means of Long, Lattm, Lt, and Kp, for all years are computed for each cell.

A "keyed" record is written on the file MONSTD to represent the standardized cell. The contents of this record include: (Key, N, Nyear, Long, Lattm, Kp, Lt, Rz, SFmin, SFmax, SA_i, SB_j, a, b), i = 1(1)10, j = 1(1)4. (See also COMPUTER OUTPUT 4, section 2.3).

The keys associated with each record are of a type associated with *direct access* READ/WRITE statements, which enable the user to directly access standardized cells upon specification of his input conditions. The keys are integers defined as a linear combination of the cell subscripts, with the weights depending on the particular cell alignment used. In this case:

$$\text{Key} = \frac{10368 (LM-1)}{12} + \frac{864 (LO-1)}{3} + \frac{288 (LA-1)}{18} + \frac{16 (LT1-1)}{2} + \frac{8 (LT2-1)}{2} + \frac{4 LK}{4}$$

or more compactly,

$$\text{Key} = 864 LM + 288 LO + 16 LA + 8 LT1 + 4LT2 + LK - 1180 \quad (2.8)$$

Thus the keys are in the range [1, 10368] with empty cells (no data) corresponding to non-existent keys. The last step in preparing the reduced data file for the model is simply to concatenate all the months together using PCL (file management system for the Honeywell computer) on a file ALLMON.

A single example is now presented.

Example 2: February: 1,5,2,1,3,2; this is a (3,5) cell (see Table 5).

Here there are 3 quality years: 1964, 1966 and 1967.

The blocked record of MONB96 appears as:

k	n _k	Long _k	Lattm _k	Lt _k	Kp _k	Fmin _k	Fmax _k	Rz _k	A _{ki}						B _{ki}								
1	18	-157.0	67.3	16.94	4.0	2.07	5.05	16.2	1	4	8	0	1	1	2	0	0	1	0	6	12	0	
2	7	-153.0	67.6	17.13	4.6	4.53	5.36	32.2	3	2	0	0	1	0	0	0	0	0	1	0	1	6	0
3	7	-153.4	67.7	17.08	4.2	2.48	8.36	75.7	2	1	0	1	0	0	0	0	1	1	1	0	4	3	0

In Figure 8(b), the median foF2 v. Rz relationship for these three years has been plotted for this cell. The standardized histogram of foF2 lies in [1.71, 7.59] with occurrence frequencies consisting of the array

2, 2, 12, 2, 3, 6, 2, 1, 1, 1

from minimum foF2 to maximum foF2.

As a consistency check it is noted that for the immediately preceding cell (lower Kp), the foF2 v. Rz relationship is even "flatter":

$$\text{foF2} = 0.019 Rz + 3.64.$$

This cell is of much better quality, (5,15), in terms of Table 5.

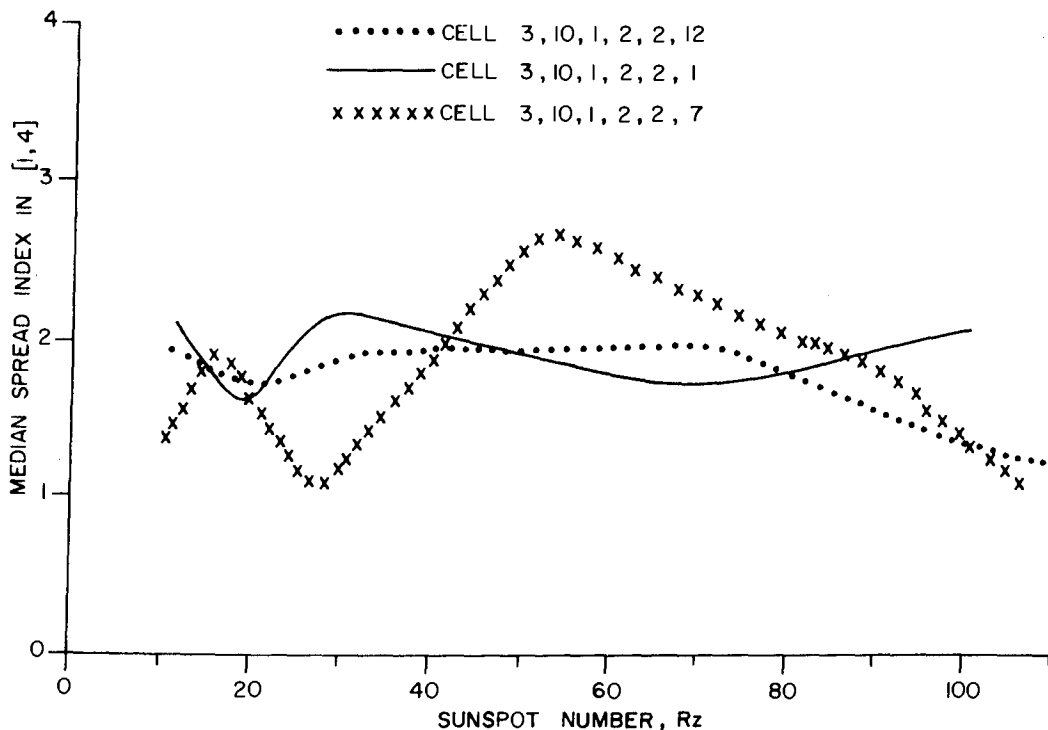


Figure 8(a). Spread Versus Sunspot Number for a Given Longitude, Latitude, Local Time, Magnetic Activity and Month.

GEOGRAPHIC LONGITUDE 154.5°W
 GEOMAGNETIC LATITUDE 67.5°N
 LOCAL TIME 1703 hrs.
 MAGNETIC ACTIVITY, Kp 4.3
 FEBRUARY
 NUMBER OF IONOGRAMS (3 yrs.) 32

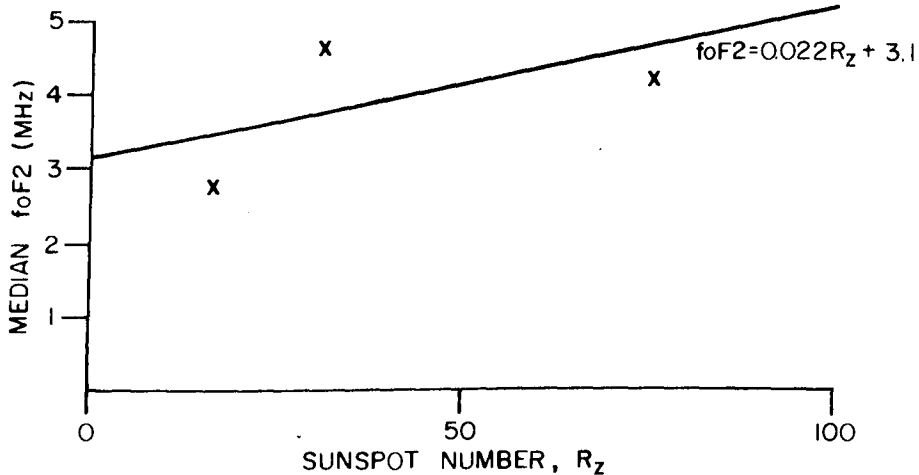


Figure 8(b). foF2 Versus Sunspot Number for a Given Longitude Latitude, Local Time, Magnetic Activity and Month.

2.3 IMPLEMENTATION OF THE MODEL

2.3.1 Real Time Accession of the Data

The reduced file, ALLMON, now exists which consists of at most 10,368 keyed records, each record representing a standardized cell. Actually about one third of these records will be "non-existent" due to empty cells over oceans areas.

Upon specification by the user of a particular point (Long, Lattg, Rz, M, Kp), the subscripts of that cell can be computed, the key computed by equation (2.8), and the cell directly accessed. Actually only the shortened equation

$$\begin{aligned} \text{Key} &= 864 \text{ LM} + 288 \text{ LO} + 16 \text{ LA} + 8(2) + 4(2) + 4 - 1180 - 16 \\ &= 864 \text{ LM} + 288 \text{ LO} + 16 \text{ LA} - 1168 \end{aligned} \quad (2.9)$$

need be used and (at most) the next 16 cells for each of the months M-1, M, and M+1. As mentioned above, 3 months are required to obtain sufficient local time coverage. See Table 6 for a display of the cell (key) structure of ALLMON. With little additional effort, one can access 5 months (i.e. also M-2 and M+2); however, unless stated explicitly otherwise, it will be assumed throughout the remainder of the chapter that 3 months have been accessed.

A few comments concerning the use of Table 6 are appropriate:

- (1) This represents the "format" for the month of January (other months are simply translations of the key by 864).
- (2) The 3 longitude zones are represented by the 3 major columns, and the 18 latitude zones by the 18 major rows.
- (3) Within one of the large blocks, the four columns represent the 4 local time zones (with indices 11, 12, 21, and 22) while the 4 rows represent the 4 Kp zones in order of increasing magnetic activity.
- (4) The contents of any cell up to cell 495 of December (Key = 11 x 864 + 495 = 9999) can be actually displayed by using the EDIT processor of the Honeywell Sigma 9 computer. For greater keys, one must resort to the KFM (keyed file manipulation) processor.

Having accessed at most 48 cells (4 Kp x 4 local time x 3 months) one must first adjust the data to the user's sunspot number, magnetic activity, and month. The values of the characteristics will actually be computed for all local times (hourly intervals).

2.3.2 Correction to the User's Rz and Kp

For each of the (at most) 48 cells the foF2 is adjusted to the user's sunspot number Rz using:

$$\text{foF2} = a(\text{Lt}, \text{M}, \text{Kp}) \text{ Rz} + b(\text{Lt}, \text{M}, \text{Kp}) \quad (2.10)$$

For the remaining characteristics (foF2 percentile, median spread, spread percentile) the following is used:

$$U_c = S_c + a(Lt, M, Kp) (Rz - \overline{Rz}) \quad (2.11)$$

where S_c is the characteristic computed from the *standardized* histogram,

\overline{Rz} is the average sunspot number of the cell,

U_c is the characteristic corrected to the user's Rz .

As discussed above $a(Lt, M, Kp)$ is taken to be zero for the spread (see Figure 8(a)).

At this point, for each of the 12 (Lt,M) pairs, there exists an array of at most 4 pairs (Kp_i, U_{c_i}) , $i = 1(1)4$, where U_{c_i} is the value of the characteristic adjusted to the user's sunspot number (if necessary). To interpolate to the user's Kp , UKp , the following is used:

$$U_c = \begin{cases} U_{c_1} & UKp \leq Kp_1 \\ P_3(U_{c_1}, U_{c_2}, U_{c_3}, U_{c_4}) & Kp_1 < UKp < Kp_4 \\ U_{c_4} & UKp \geq Kp_4 \end{cases} \quad (2.12)$$

where P_3 is the Lagrange interpolation polynomial of degree 3 through the 4 points. If there are less than 4 such pairs (due to non-existent cells or "missing" Rz coefficients a, b) the degree of the Lagrange interpolation is appropriately reduced. If the number of points available is zero, there will be less than 12 triples to be used in interpolation in the next section. In such a case, the user is informed and the interpolation procedure in section 2.3.3 is omitted. However, the user can obtain the available triples (< 12).

2.3.3 Interpolation to Month and Local Time

The 12 triples (M_i, Lt_i, U_{c_i}) , $i = 1(1)12$, corresponding to the 6 half-months of data with 2 periods of local time each are used in a least squares model to obtain an array of the characteristic at the middle of the user's month and for each hour of local time. The variable used to describe the monthly variation is

$$W_i = \begin{cases} i & i \text{ is odd} \\ i-1 & i \text{ is even} \end{cases}$$

Thus it is essentially assumed the data for a given half month occur at the middle of the half month. The form of the model to fit the data is:

$$U_c(Lt, W) = b_0 + \sum_{j=1}^4 b_{2j-1} (\sin \pi Lt/12)^j + b_{2j} (\cos \pi Lt/12)^j + \sum_{j=1}^3 b_{j+8} (W/12)^j \quad (2.13)$$

W in $[1, 12]$; Lt in $[0, 24]$

The subroutines STEP1 and STEP2 perform a stepwise regression procedure for calculating and selecting the statistically significant (non-zero) coefficients $b_j; j=0(1)11$. See also Ralston and Wilks [24] or Frazer [8]. These subroutines require a pair of parameters (F1,F2) which are used for entering and removing a given variable in the model (2.13). Typical values of F1 and F2 are about 5 for a 95% level of significance.

2.3.4 Illustration

A display of the results of the main prediction program, PREDSYS, is now given where the user has input the conditions:

Long = 67°W, Lattg = 45°N, Rz = 30, Kp = 1+, M = 2

He also desires a 90% - tile for each of the characteristics. See COMPUTER OUTPUT 2 for an example of the actual execution procedure.

In COMPUTER OUTPUT 3, the foF2 (MHz), spread, and slab thickness (km) are listed for each hour of local time. Finally, in COMPUTER OUTPUT 4, the actual cells of ALLMON (directly accessed in the above predictions) are displayed. See remark 4 in section 2.3.1.

In Table 7, the actual (significant) regression coefficients of (2.13) as well as the Root Mean Square Deviation of the estimates are displayed, for each of the 4 characteristics, corresponding to the set of predictions in COMPUTER OUTPUT 3. The empirical model for slab thickness is described in Chapter 3.

In Figures 9(a), 9(b), and 9(c) contour maps of foF2, spread and slab thickness are displayed for the above input conditions, including all northern latitudes.

In conclusion, the following remarks are made:

- (1) The Root Mean Square Deviation (in Table 7) is only strictly applicable to the deviations between the actual (12) observed values of a characteristic and the calculated values using (2.13). However these deviations should approximately apply for any predictions $U_c(Lt,W)$ in view of the natural continuity of the characteristic, in local time and month.
- (2) The accuracy of estimates (and even the capability of prediction) is dependent on the number of ionograms available in the various cells directly accessed. Inspection of the data totals, for a typical month, (see Table 4) suggests the following real spatial domain, D , for the model.

$$D = (A1 \times A2) \cup (B1 \times B2) \cup (C1 \times C2) \quad (2.14)$$

where $A1, A2, B1, B2, C1$ and $C2$ are the sets:

$A1 : [180^\circ W, 135^\circ W]$

$A2 : [45^\circ N, 90^\circ N]$

B1 : [135°W, 90°W]

B2 : [30°N, 90°N]

C1 : [90°W, 45°W]

C2 : [0° , 90°N]

The first set of each pair, in (2.14), is the longitude range; the second is the geomagnetic latitude range.

In addition the sunspot number range is restricted to $R_z \leq 112$ (Table 3) although there is some evidence [6] that foF2 is independent of R_z for $R_z > 150$. A more serious limitation is that approximately two thirds of the data is in the low sunspot number range (Table 2)

- (3) One could directly access 5 months of data with little extra effort by redefining the size of the arrays in PREDSYS. This would yield at most 20 triples of observations to be used in the

TABLE 7

Illustration of Significant Regression Coefficients in Equation (2.13)

i		COEFFICIENT b_i			
		foF2	foF2 %	SPREAD	SPREAD %
0	CONSTANT	3.3842	4.1832	2.0866	2.4575
1					
2	L	-2.1063	-1.9051		
3	O				0.49167
4	C				
5	A				
6	L				
7	T	-1.5679	-1.7373		
8	I				
9	M				
10	O			0.076441	
11	N				
	T		2.7504		
	H	1.9931			
				-0.18646	
	ROOT MEAN SQUARE DEVIATION	0.61	0.64	0.05	0.18

COMPUTER OUTPUT 2. Example of Control Procedure Required for Predictions

```
.EXAMPLE SET OF PREDICTIONS USING EXPREDSYS
!.FOR LONGITUDE=67 W(DEGREES),LATITUDE=45 N(DEGREES)
!.RZ=30,FEBRUARY,KP=1+
!XEQ EXPREDSYS,36
  0036 - !.
  0037 - !.A FILE NULL IS BUILT CONSISTING OF A SINGLE RECORD.
  0038 - !.NAMELY THE 2 CHARACTERS !.
  0039 - !.THIS IS USED TO BREAK THE EXECUTION AFTER THE
  0040 - !.USER OBTAINS HIS CONTOUR DATA,ON UNIT 80,TO
  0041 - !.BE USED FOR EDITING . AFTER HE COMPLETES THE
  0042 - !.TASK,HE CAN RESUME EXECUTION AT THE LINE 91
  0043 - !.FOR CONTOUR PRODUCTION.
  0044 - !B NULL
1.000 !.
2.000
  0045 - !.
  0046 - !.THE OLD GRID OF CONTOUR DATA IS DELETED.
  0047 - !.
  0048 - !DELETE NEWPLOT1
          $
0300 FILE DOES NOT EXIST.
  0049 - !SET F:105 ME;IN
  0050 - !SET F:6/ALLMON;IN;KEYED;DIRECT
  0051 - !SET F:7 ME;OUT
  0052 - !SET F:80/NEWPLOT1;OUT;KEYED;DIRECT
  0053 - !SET F:70/ADJRZ;OUT
  0054 - !SET F:71/ADJKP;OUT
  0055 - !SET F:108/REGFIT;OUT
  0056 - !LYNX BPREDSYS,BMISC,BSSTEP1,BSSTEP2
:P1 ASSOCIATED.
GROUPC2 OF :LIB.:SYS ASSOCIATED FOR POSREC
GROUP04 OF :LIB.:SYS ASSOCIATED FOR SQRTF
GROUP21 OF :LIB.:SYS ASSOCIATED FOR 9DEFIL
GROUP23 OF :LIB.:SYS ASSOCIATED FOR 7ERRARG
GROUP14 OF :LIB.:SYS ASSOCIATED FOR 9IFR
GROUP17 OF :LIB.:SYS ASSOCIATED FOR 9INPUTL
  ** ALLOCATION SUMMARY **
PROTECTION      LOCATION  PAGES
DATA (00)        A000      9
PROCEDURE (01)   B600     10
DCB (10)         B200      2
  0057 - !.
  0058 - !.ST GIVES CURRENT CPU TIME CONSUMED.
  0059 - !.
  0060 - !ST
```

COMPUTER OUTPUT 3. Example of Predictions Using Control Procedure of COMPUTER OUTPUT 2

CPU = .1505 CON= 00:19:03 INT = 25 CHG = \$.94 CALS = 1255
0061 - !S

SPECIFY YOUR LOCATION...EXAMPLE, FOR OTTAWA....

-75.0, 45., 56, 2, 1.7, .95, .75, ... MEANS

GEOGRAPHIC LONGITUDE IS 75W(DEGREES).

GEOGRAPHIC LATITUDE IS 45N(DEGREES).

SUNSPOT NUMBER IS 56...IF SUNSPOT NUMBER IS

> 150, ENTER 150 AS THE CHARACTERISTICS ARE

ASSUMED INDEPENDENT OF IT IN THAT DOMAIN.

MONTH IS FEBRUARY, IE MIDPOINT OF THE MONTH

3-HOURLY KP IS 2-.

A 95 %-TILE OF FOF2 IS DESIRED.

A 75 %-TILE OF SPREAD IS DESIRED.

ALL CHARACTERISTICS ARE COMPUTED FOR EACH

HOUR OF LOCAL TIME...INCIDENTALLY, A 95%-TILE

IS THE VALUE OF THE CHARACTERISTIC SUCH THAT

95 % OF THE DATA IS LESS THAN THAT VALUE.

FOF2 IS IN MHZ...SLAB THICK IS IN KM

TO STOP, ENTER 1000, 0, 0, 0, 0, 0, 0.

ALSO USE THIS AS THE LAST RECORD OF AN INPUT FILE

OF CONDITIONS...IE WHEN PREPARING CONTOUR MAPS.

SEE COMMENT STATEMENTS IN SOURCE PROGRAM ABOUT

PREPARING CONTOUR MAPS.

?-67, 45, 30, 2, 1.3, .9, .9

THERE ARE 12 TRIPLES OF LOCAL TIME AND MONTH DATA

IF LESS THAN 12, TRY AN ADJACENT CELL...OR DIRECTLY

ACCESS THE CELLS USING EDIT OR KFM PROCESSORS.

THE PRELIMINARY INTERPOLANTS ARE ON UNITS 70 & 71

GEOGLONG= -67.0 GEOGLAT= 45.0 SUNSPOT= 30.

MONTH= 2 KP=1.3

PROB FOF2= .90 PROB SPREAD= .90

GEMATLAT=56.4

LOCAL TIME	FOF2	FOF2%	SPREAD	SPREAD%	SLAB	THICK
0	1.5	3.0	2.0	2.5		181.
1	1.6	3.0	2.0	2.5		175.
2	1.6	3.0	2.0	2.6		178.
3	1.6	2.9	2.1	2.7		193.
4	1.6	2.8	2.1	2.8		213.
5	1.7	2.8	2.1	2.9		231.
6	2.1	3.1	2.1	2.9		238.
7	2.8	3.8	2.1	2.9		231.
8	3.7	4.7	2.1	2.8		213.
9	4.6	5.6	2.0	2.7		193.
10	5.3	6.3	1.9	2.6		178.
11	5.6	6.7	1.9	2.5		175.
12	5.7	6.8	1.8	2.5		181.
13	5.7	6.7	1.9	2.5		192.
14	5.7	6.7	1.9	2.6		201.
15	5.7	6.8	2.0	2.7		202.
16	5.7	7.0	2.1	2.8		198.
17	5.6	6.9	2.1	2.9		192.
18	5.2	6.6	2.1	2.9		189.
19	4.5	5.9	2.1	2.9		192.
20	3.6	5.0	2.1	2.8		198.
21	2.7	4.1	2.1	2.7		202.
22	2.0	3.4	2.0	2.6		201.
23	1.6	3.1	2.0	2.5		192.
24	1.5	3.0	2.0	2.5		181.

?1000, 0, 0, 0, 0, 0, 0

STOP 0

COMPUTER OUTPUT 4. Extract From the File ALLMON

Key	Cell Indices	N	Long	Lat	X	Kp	Lt	Rz	foF2 (min)	foF2 (max)	CpF2 Distribution	a	b																
EDIT ALLMON																													
*ALLMON:2B420IR:FILE NOT CREATED BY EDIT (KEYH NOT 3)																													
*TY673-688																													
673.000	3 7111	1 37	4	-72.2	57.4	146	.52	22.16	53.42	1.18	3.53	3	0	5	3	2	7	6	8	2	1	0	34	3	0	.0359	.7917		
674.000	3 7112	1 25	3	-72.6	57.8	146	2.47	22.27	63.63	1.23	4.27	1	0	3	1	2	0	2	6	9	1	1	24	0	0	.0344	1.0889		
675.000	3 7113	1 16	4	-78.3	57.5	144	4.32	21.96	32.87	1.64	2.21	9	0	1	2	0	0	0	0	0	0	4	10	5	0	.0005	1.7821		
676.000	3 7114	1 13	1	-69.4	57.8	141	7.00	21.75	72.30	3.34	5.01	1	1	3	0	2	2	0	0	0	1	3	17	5	0	.0000	.0000		
677.000	3 7121	1 106	6	-70.0	57.6	82	.72	8.80	43.45	2.78	7.27	3	0	1	7	0	0	23	40	16	11	2	77	27	0	.0623	3.0773		
678.000	3 7122	1 87	6	-76.5	57.4	83	2.57	8.65	43.45	1.78	7.74	3	4	7	0	0	0	21	31	8	1	5	5	72	10	0	.0682	2.5767	
680.000	3 7123	1 32	4	-72.7	57.5	82	4.25	8.76	54.95	3.04	6.87	1	1	1	1	4	6	1	4	2	0	1	4	2	7	5	.0512	1.6917	
681.000	3 7124	1 5	1	-76.5	57.2	85	5.70	8.73	72.30	4.85	5.57	1	2	0	0	0	0	0	1	0	1	0	4	1	0	0	.0000	.0000	
682.000	3 7211	1 73	5	-77.1	57.7	123	2.36	20.10	54.95	2.09	5.56	1	13	15	4	5	12	4	8	6	5	1	63	9	0	.0490	.6612		
683.000	3 7212	1 13	3	-67.2	57.4	123	4.37	20.09	49.17	1.63	4.91	2	10	12	3	2	1	5	14	2	5	14	2	1	54	18	0	.0305	1.7524
685.000	3 7221	1 50	4	-72.7	57.4	100	.97	6.52	54.95	1.69	4.43	1	0	2	3	2	1	0	0	1	0	0	1	2	11	0	.0427	.7250	
686.000	3 7222	1 33	3	-75.2	57.3	93	2.33	7.27	67.20	1.48	4.64	2	0	9	1	8	2	0	0	0	1	3	37	10	0	.0302	.8155		
687.000	3 7223	1 15	2	-75.2	57.0	96	4.05	6.93	23.55	1.18	3.74	3	0	2	2	1	1	0	0	1	0	0	1	5	0	0	.0195	1.8773	
February																													
*TY1537-1552																													
1537.000	3 7111	2131	6	-68.7	57.7	100	.62	18.21	44.57	4.13	6.76	2	8	6	16	15	19	31	10	20	4	13	81	37	0	.0613	2.7707		
1538.000	3 7112	2140	6	-68.4	57.6	96	2.33	17.82	44.57	4.50	8.96	4	19	27	40	30	7	2	4	2	5	14	95	31	0	.0585	3.4273		
1539.000	3 7113	2 26	4	-71.7	57.4	100	4.05	18.14	38.50	3.50	6.11	1	2	5	1	4	1	4	7	0	1	4	14	8	0	.0537	2.9366		
1540.000	3 7114	2 8	2	-72.0	57.4	99	6.00	18.07	45.95	2.41	6.40	3	2	2	0	0	0	0	0	0	0	1	0	6	2	0	.03F1	1.2703	
1541.000	3 7121	2 44	4	-75.4	57.1	116	.82	4.74	33.47	.58	3.36	1	0	3	10	9	14	6	0	0	1	2	33	9	0	.0312	.8215		
1542.000	3 7122	2 45	3	-79.9	57.8	115	2.43	4.77	64.40	1.69	4.78	1	6	12	8	4	5	0	3	2	2	41	2	0	0	.0292	.9265		
1543.000	3 7123	2 20	4	-73.3	58.2	118	4.20	4.45	55.77	1.87	3.46	2	6	1	0	0	0	0	0	0	2	2	4	1	2	0	.0143	1.6723	
1544.000	3 7124	2 15	2	-64.6	57.3	119	5.85	4.42	55.60	2.55	3.80	3	1	0	0	0	0	0	0	0	4	7	0	13	2	0	.0294	1.7041	
1545.000	3 7211	2168	6	-69.5	57.6	78	2.23	16.26	44.57	5.95	8.90	6	20	20	21	49	27	6	11	3	5	26	106	36	0	.0673	4.2767		
1546.000	3 7212	2121	6	-62.3	57.5	78	4.52	16.22	47.50	5.08	8.46	1	0	1	1	6	10	8	16	0	4	6	19	84	18	0	.0605	4.3707	
1547.000	3 7213	2 47	5	-70.7	57.5	72	4.52	16.22	47.50	5.08	8.46	1	0	1	1	6	10	8	16	0	4	6	19	84	18	0	.0617	4.3660	
1548.000	3 7214	2 4	1	-58.6	57.2	72	5.70	15.70	16.20	5.69	6.31	2	4	14	14	2	3	1	0	0	0	3	0	4	0	0	.0000	.0000	
1549.000	3 7221	2 47	4	-70.2	57.7	128	.85	3.13	54.75	1.23	4.57	2	4	14	14	2	3	1	0	6	1	0	34	13	0	.0274	.8334		
1550.000	3 7222	2 65	4	-75.9	57.3	129	2.22	3.06	51.32	.66	4.84	1	10	18	15	4	2	2	10	2	1	3	56	6	0	.0210	.9226		
1551.000	3 7223	2 18	3	-70.0	57.7	128	4.50	3.05	64.40	1.44	4.17	1	0	2	2	4	1	3	3	3	1	1	0	18	0	0	.0114	2.2443	
*TY2401-2416																													
March																													
2401.000	3 7111	3172	6	-69.0	57.7	58	.82	14.26	45.48	5.20	9.13	7	3	7	19	51	24	8	25	19	9	26	139	7	0	.0648	4.4536		
2402.000	3 7112	3176	6	-68.7	57.6	57	2.40	14.14	45.48	4.64	9.62	11	1	6	29	28	22	14	20	21	7	23	140	13	0	.0474	5.0781		
2403.000	3 7113	3 18	3	-72.4	57.1	58	4.47	14.24	48.40	4.57	7.90	2	3	0	2	2	4	0	0	0	5	2	11	5	0	.0000	.0000		
2404.000	3 7114	3 5	1	-69.8	57.8	55	6.00	13.91	29.00	5.06	5.57	4	0	0	0	0	0	0	0	0	0	1	0	0	5	0	.0000	.0000	
2405.000	3 7121	3 60	3	-77.5	57.6	136	.63	1.11	65.27	.30	5.14	2	0	2	0	0	0	5	9	0	35	7	0	54	0	0	.0381	1.2054	
2406.000	3 7122	3 61	4	-75.7	57.4	136	2.55	1.01	56.20	.38	4.77	3	0	0	8	11	15	7	4	4	9	7	54	0	0	.0276	1.2087		
2407.000	3 7123	3 12	4	-73.3	57.7	137	3.92	.97	39.75	1.28	3.87	1	0	1	2	1	4	2	0	0	1	1	11	0	0	.0324	1.3321		
2409.000	3 7211	3140	6	-66.9	57.6	45	.90	12.25	45.48	5.06	9.46	5	2	10	15	35	34	18	11	3	7	58	67	15	0	.0551	4.8052		
2410.000	3 7212	3153	6	-67.4	57.7	46	2.32	12.42	45.48	4.43	10.08	8	2	15	28	31	18	25	10	9	7	21	112	20	0	.0424	5.3758		
2411.000	3 7213	3 32	3	-67.4	57.6	44	4.17	12.07	50.63	4.92	9.22	1	4	6	4	2	0	0	0	3	6	6	5	23	4	0	.0293	5.7216	
2412.000	3 7214	3 19	3	-73.6	57.8	46	6.00	12.50	42.33	5.14	8.51	4	0	2	6	3	0	1	0	1	0	1	15	4	0	.0659	3.3405		
2413.000	3 7221	3 59	5	-73.4	57.8	129	.56	22.91	47.58	2.08	5.64	1	2	1	7	11	10	6	6	9	6	8	47	4	0	.0527	1.3393		
2414.000	3 7222	3 79	5	-73.5	57.7	128	2.50	22.79	48.78	.75	6.94	2	4	9	18	13	4	6	10	12	1	3	69	7	0	.0303	2.4651		
2415.000	3 7223	3 25	3	-74.5	58.0	131	4.23	23.31	65.27	.84	5.72	2	2	6	1	3	6	0	4	0	1	3	22	0	0	.0245	1.5909		

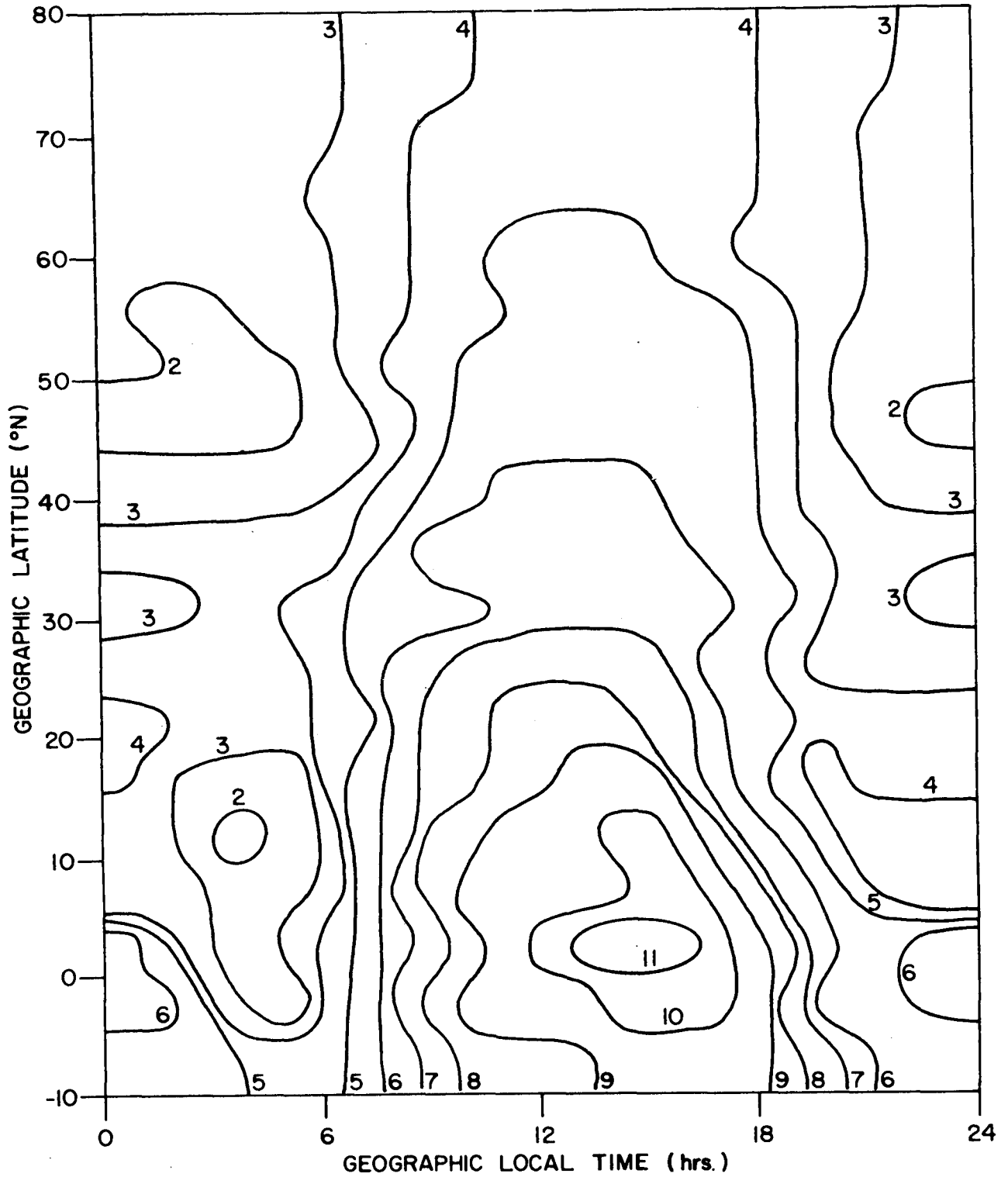


Figure 9(a). Contours of Characteristics in Latitude and Local Time, foF2 (MHz).

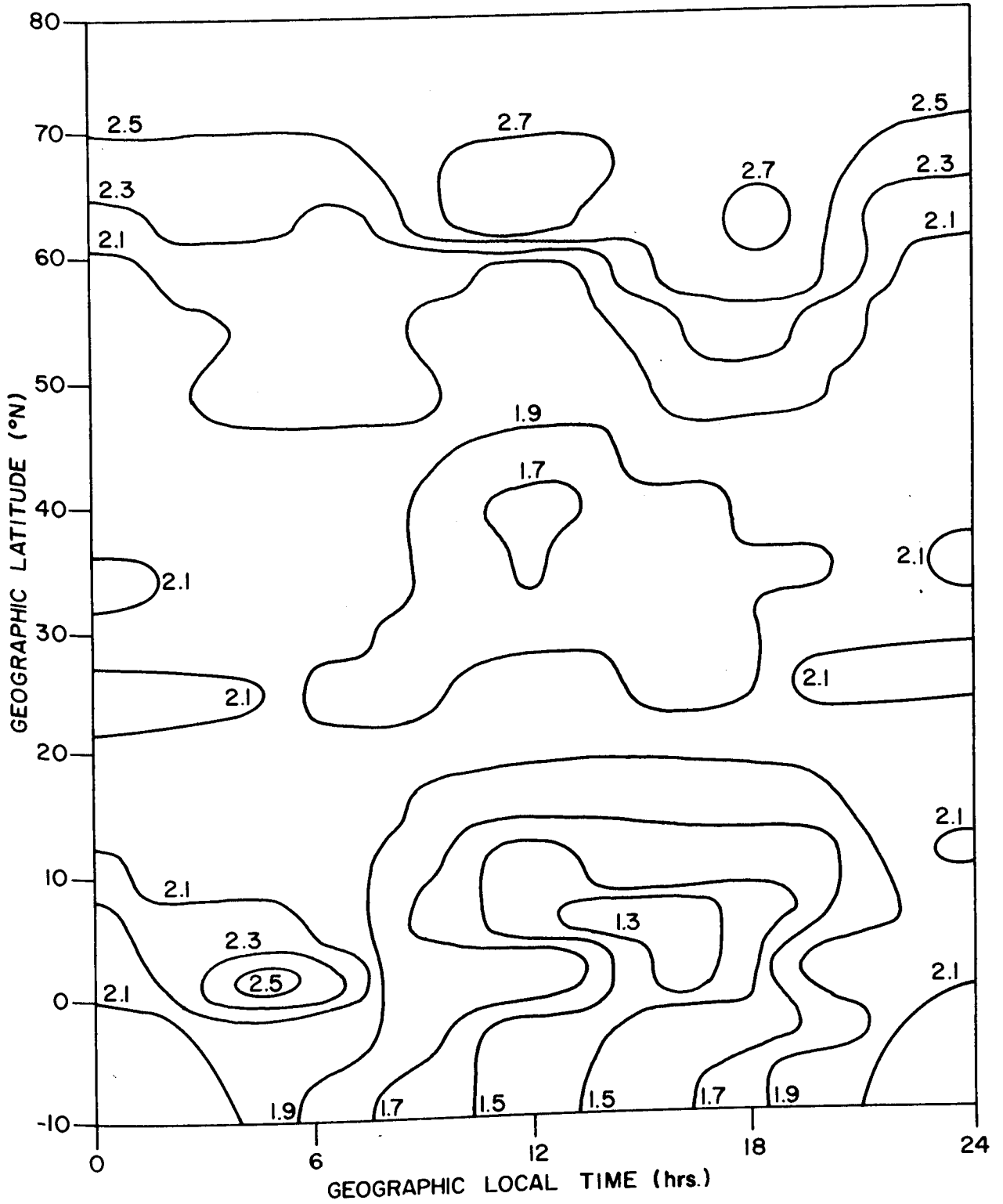


Figure 9(b). Contours of Characteristics in Latitude and Local Time, spread in [1,4].

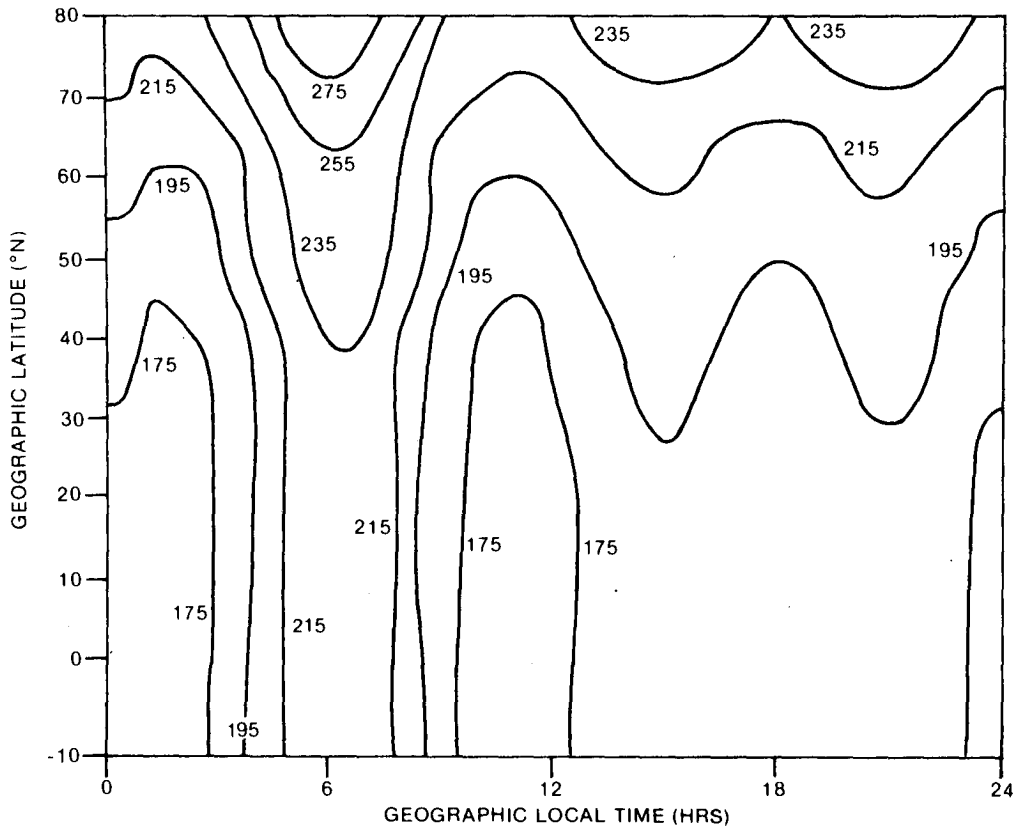


Figure 9(c). Contours of Characteristics in Latitude and Local Time, Slab Thickness (km).

determination of the model (2.13). Balanced against this, there would be more monthly variation to be described by the model.

- (4) The current cell alignment, for a given month, leads to a prolific number of cells with few ionograms (especially for those corresponding to high magnetic activity). Perhaps only 2 Kp zones, or a single zone for all Kp's would **ameliorate** this situation. A "smoothed bi-weekly Kp average" could be attached to each of the resulting 216 (= 864/4) cells. To consider such questions one only needs to apply ACCMONB96 which operates on the file MONB96 (blocked cells, but unstandardized). These files have been stored on magnetic tape (all months); see Appendix A (listing of tapes).

3. N(h) MODEL

3.1 DESCRIPTION OF THE DATA BASE

About 80,000 Alouette 1 and 2 ionograms have been scaled to produce almost complete topside electron density profiles. These profiles have been

stored on 16 9-track tapes. Alouette 2 was launched in November 1965, and unlike Alouette 1 it had an elliptical orbit: apogee = 3000 km, perigee = 500 km. Since the ionograms were scaled on demand they were actually stored on tape as the need arose, resulting in a very fragmented data base, unlike ALOSYN. Indeed, the actual details of the reduction procedure [11], to generate $N(h)$ profiles, was varied throughout the years.

In Table 8 a summary of the data totals of the various tapes over the years is presented. Some remarks pertaining to this table follow.

- (1) The ionograms within a volume are in chronological order (as they were scaled).
- (2) In A Format, the electron density profiles have been calculated by assuming f_N , the plasma-frequency, is linear in height on each lamination.
- (3) In B Format, the reduction has been achieved by assuming the log of the electron density varies parabolically in each lamination (but linearly in the first lamination nearest the satellite).
- (4) The profiles tabulated by the Ames Research Centres (AMES) are actually interpolated to give electron densities at every one hundred kilometres from the height of the satellite. In addition they distinguish between field-aligned and non field-aligned profiles.
- (5) The topside TEC, in A Format, was calculated by integrating (exactly) the model electron density, $N(h)$, from the height of the satellite to a height of maximum electron density. The latter was calculated by passing a parabola through the lowest 2 scaled points and assuming foF2 was 0.01 MHz greater than the lowest scaled f_N . Thus, the topside TEC has been adjusted to include only the area to the last scaled point; the remainder of the TEC (bottomside) will be computed from the model to be described in section 3.2.2. In B Format, the topside TEC was computed to the lowest scaled point, assuming the electron density is linear on each lamination. The Ames profiles do not give TEC so a value consistent with the B Format profiles was calculated and put on tape.

There also exist 10 tape volumes of ISIS 1 and 2 profiles in B Format. These two satellites are similar to Alouette 2 and 1, respectively, in orbital configuration. They were launched in 1969 and 1971 during a decreasing period of solar activity. Thus, the data reduction procedures to be described below are readily adaptable to these data as well.

3.2 DEVELOPMENT OF THE MODEL

3.2.1 Organization of the Data Base

The intention of this section is the construction of a chronological ordered data base of the $N(h)$ profiles. Each profile of this new base will

TABLE 8
N(h) Profile Data Available

TAPE VOLUME	SATELLITE	FORMAT	ERA	NUMBER OF IONOGRAMS
1 - 4	ALOUETTE 1	A	1962 - 66	43700
5 - 7	ALOUETTE 1	B	1963 - 70	18400
1 - 5	ALOUETTE 2	B	1965 - 72	12000
6 - 9	ALOUETTE 2	AMES	1966 - 72	5200
1 - 5	ISIS 1	B	1969 - present	35000
1 - 5	ISIS 2	B	1971 - 78	43000

consist of the identification parameters (time, location, Kp, and Rz) together with certain profile characteristics, e.g. TEC (topside), TEC (bottomside), hmax, and slab thickness. The definition of these characteristics will be considered in more detail in the next section. This new data base, ALOUETTE NH, will then be similar to ALOSYN, although not nearly as extensive of course. Thus, the entire procedure of Chapter 2, with a necessarily coarser grid, can be applied to ALOUETTE NH.

An illustration of this approach will be given in section 3.2.4, for a selection of 10,000 Alouette 1 profiles (1965-70) which cover (sparsely) a half solar cycle, i.e. Rz in [12, 112] (see Table 3). The empirical model used for slab thickness, in COMPUTER OUTPUT 2, will also be fitted to these data.

The process of constructing ALOUETTE NH consisted of processing (calculating the frequency and heights, calculating the topside TEC, and attaching the Kp) for each of the 16 volumes, described above, one at a time. The resulting 16 output files were concatenated, sorted chronologically, and blocked (at the rate of 10 profiles per record). Only profiles in the longitude range $[-180^\circ, -45^\circ]$ are included in ALOUETTE NH. However, due to the small data base, all geomagnetic latitudes are included, and it is assumed that slab thickness is symmetric about the geomagnetic equator.

The data actually kept for a particular profile of ALOUETTE NH are as follows:

Volume (tape number of original profile of ALOUETTE N(h); see Table 8)

Kp (integer part only)
 Dip (dip angle at the satellite, degrees)
 Job (see below)
 Year, Day, Hour, Minute, Second (Universal time)
 TTEC (topside TEC from h_o to h_L in electrons/cm², where h_o is the satellite height and h_L is the lowest height of the topside profile)
 L+1 (number of pairs of points for profile)
 f_H (gyrofrequency at h_o , MHz)
 Long (degrees)
 Lattg (degrees)
 χ (Solar angle at satellite, degrees)
 f_N (a 4x1 vector, plasma frequency at h_o , h_{L-2} , h_{L-1} , and h_L , MHz)
 h (a 4x1 vector, real height h_o , h_{L-2} , h_{L-1} , and h_L , km)

The Job parameter is a subjective index concerning the quality of the profile on a scale of 4 (excellent) to 9 (scaled under protest). In the case of the Ames profiles, this parameter was used here to indicate whether the profile is field aligned or not.

$$\text{Job} = \begin{cases} 0 & , \text{ non field-aligned} \\ \text{Year} & , \text{ field-aligned} \end{cases}$$

In the field-aligned case, the longitude and latitude are the arithmetic means of the longitudes and latitudes of the various points along the magnetic field direction.

3.2.2 Definition of the Profile Using ALOUETTE NH

Here, a method of defining a parabola will be outlined, using the data of ALOUETTE NH, to represent the profile from h_L down to h_p , a base for a hypothetical F2 layer to be defined below. From this parabola, rough estimates of the bottomside total electron content (BTEC), h_{max} , and slab thickness can be made. High quality estimates will also be compared with an alternative method (for limited samples of data) using ground echoes. High quality ground echoes usually only occur on the Alouette ionograms from soundings taken over water or over less densely populated areas where noise levels are low. This fact, combined with the additional scaling effort that would be required, precludes the use of this method for the entire data base.

The first step is to define certain subsets of ALOUETTE NH consisting of "quality" profiles. Here, quality means that the last point (N_L, h_L) is "reasonably close" to the peak electron density (N_{max}, h_{max}). The electron density N is related to the plasma frequency f_N at any height, h , by

$$N = 1.24 \times 10^4 \times f_N^2 \quad (3.1)$$

where N is in electrons/cm³, f_N is in MHz. Usually the profiles from topside soundings tend to be too low [12]. However, Jackson [12] notes that they can also be high (particularly for soundings when the satellite is above 2000 km). To define the subset of quality profiles some weak conditions will be imposed on the pairs of points, rather than simply relying on the subjective job index. Before enumerating these restrictions, a comparison of the f_N at $h=h_L$ and foF2, obtained from ALOSYN, for some selected ionograms is given.

In Table 9, Δ is defined as:

$$\Delta = 100 [f_{oF2} - f_N(h_L)] / f_N(h_L) \quad (3.2)$$

From this Table, the median Δ is between 0 and 2, i.e. foF2 exceeds $f_N(h_L)$ by 2% on average. Also about 85% of the data are such that $\Delta < 5$. These profiles should comprise the quality subset.

TABLE 9

Comparison of Lowest Scaled $N(h)$ Profile Point and foF2 From ALOSYN for Selected Passes

Δ	CUMULATIVE PROBABILITY DISTRIBUTION OF Δ			
	FEBRUARY 1965 $R_z = 12$	APRIL 1965 $R_z = 12$	FEBRUARY 1967 $R_z = 76$	APRIL 1967 $R_z = 81$
-6	4	1	7	1
-5	5	2	8	3
-4	6	3	9	3
-3	7	5	10	3
-2	11	6	16	3
-1	18	11	21	11
0	25	16	26	27
1	51	37	53	61
2	65	52	61	83
3	76	68	73	89
4	82	79	78	92
5	88	88	83	96
6	91	90	86	96
7	93	92	87	97
8	94	93	89	97
9	95	96	90	100
10	96	96	90	100
NUMBER OF IONOGRAMS	589	275	263	71

The weak restrictions for defining the quality subset of ALOUETTE NH are now enumerated:

$$(1) \quad N_o (h_o - h_L) \leq \int_{h_L}^{h_o} N(h) dh \leq \frac{N_o + N_L}{2} (h_o - h_L)$$

$$(2) \quad N_{L-2} < N_{L-1} < N_L ; \quad h_{L-2} > h_{L-1} > h_L$$

$$(3) \quad h_o < 2000$$

$$(4) \quad h_b < h_L < 600$$

For the base of the layer, h_b , at which $N_b=0$, the following heuristic model based on experience [E.L. Hagg, private communications, 1978] has been used:

$$h_b = \begin{cases} 2.5 Lt + 230 & , Lt \text{ in } [0,4] \\ 30\sin(\pi Lt/8) + 210 & , Lt \text{ in } [4,12] \\ 180 \exp [0.0204(Lt-12)] & , Lt \text{ in } [12,24] \end{cases} \quad (3.3)$$

where Lt is local time in hours, and h_b is in km.

An empirical model for the height of maximum electron density of the F1 layer [25], given by

$$h_{\max} F1 = 165 + 0.6428 \chi, \quad (3.4)$$

is compared with (3.3) in Figure 10 (χ is in degrees).

The complete density profile is summarized in Figure 11. A few remarks are added:

- (1) The following artifice will be convenient. For the exponential function

$$N = N_1 \exp[(h-h_1)/H] \quad (3.5)$$

passing through any 2 points (N_2, h_2) and (N_1, h_1) (with N in $[N_2, N_1]$ and h in $[h_1, h_2]$),

$$H = (h_1 - h_2) / \ln(N_1/N_2) < 0 \quad (3.6)$$

is called effective scale height. Note that the symbols in (3.5) and (3.6) are generic; they will be specified in (2) and (3) below.

- (2) In a few cases, i.e. for Alouette 2, the satellite is considerably below 1000 km. In such cases, an exponential curve is passed

———— HEIGHT AT BASE OF F2 LAYER (h_b)

- - - - HEIGHT OF MAXIMUM DENSITY OF
F1 LAYER ($h_{max. F1}$)

JUNE, GEOGRAPHIC LATITUDE $40^\circ N$

..... HEIGHT OF MAXIMUM DENSITY OF
F1 LAYER ($h_{max. F1}$)

DECEMBER, GEOGRAPHIC LATITUDE $40^\circ N$

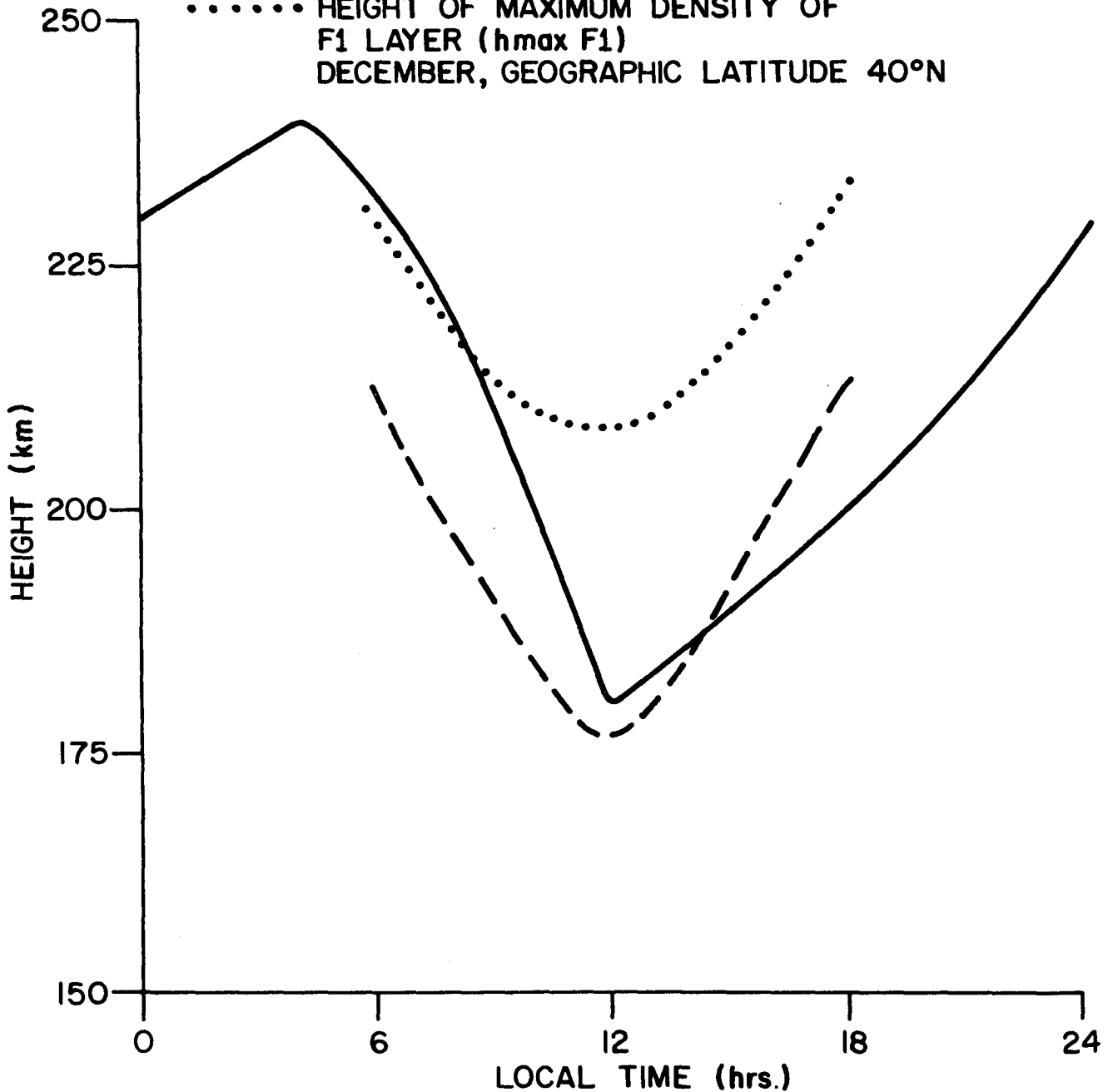


Figure 10. Height of the Base of the F2 Layer Versus Local Time

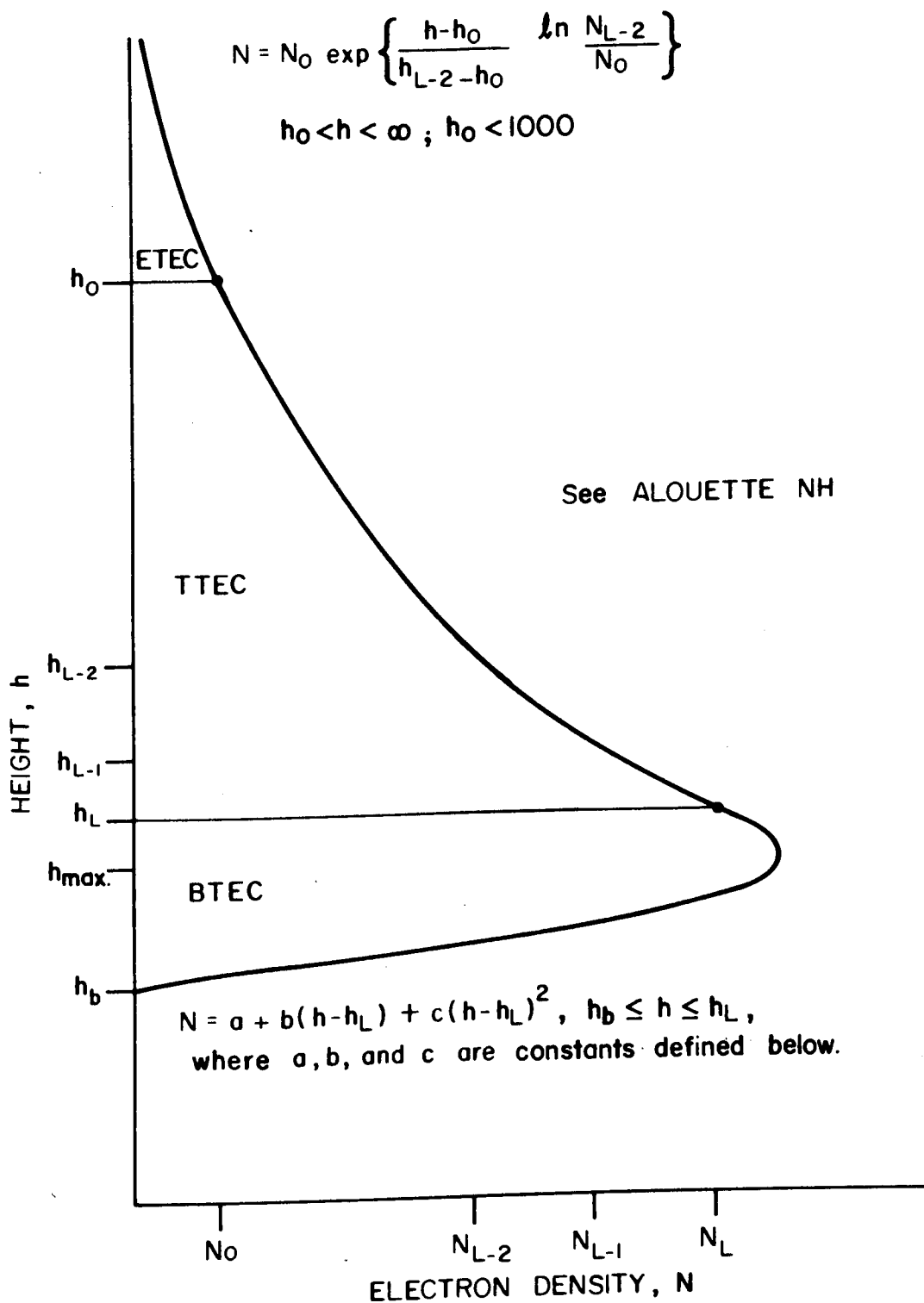


Figure 11. Summary of the Model $N(h)$ Profile

through the points (N_0, h_0) and (N_{L-2}, h_{L-2}) , in order to make a correction for the total electron content above the satellite. This extra area is:

$$\text{ETEC} = \int_{h_0}^{\infty} N(h) dh = -N_0 H \quad (3.7)$$

- (3) The constants of the parabola are chosen in order that it is continuous and has a continuous slope at (N_L, h_L) . The slope of

$$N = N_L \exp [(h-h_L)/H]$$

at $h = h_L$ is used for this purpose, where H is a scale height for the exponential on $[h_L, h_{L-1}]$. The third requirement is that $N(h_b) = 0$ where h_b is the base of the layer, as previously defined. Thus the parabola, illustrated in Figure 11, is

$$N = N_L \left\{ 1 + \frac{h - h_L}{H} - \left(1 + \frac{h_b - h_L}{H} \right) \left(\frac{h - h_L}{h_b - h_L} \right)^2 \right\} \quad (3.8)$$

Setting $N'(h) = 0$, in (3.8)

$$h_{\max} = h_L - (b/2c) \quad (\text{note } b, c < 0 \text{ since } H < 0 \text{ and } h_b < h_L) \quad (3.9)$$

$$N_{\max} = a + b(h_{\max} - h_L) + c(h_{\max} - h_L)^2 \quad (3.10)$$

Finally

$$\text{BTEC} = \int_{h_b}^{h_L} N(h) dh \quad (3.11)$$

and slab thickness is

$$Th = (\text{ETEC} + \text{TTEC} + \text{BTEC})/N_{\max} \quad (3.12)$$

3.2.3 Definition of Profile Using Ground Echoes

In this section, an alternative approach for estimating profile characteristics by adapting an idea of Dyson [7] to the present data base will now be outlined. The method essentially is an attempt to model a complete profile (topside and bottomside) using only data available from satellite soundings.

For frequencies, f_x , at which ground echoes occur the group path due to ionization below h_L is given by (see Figure 12)

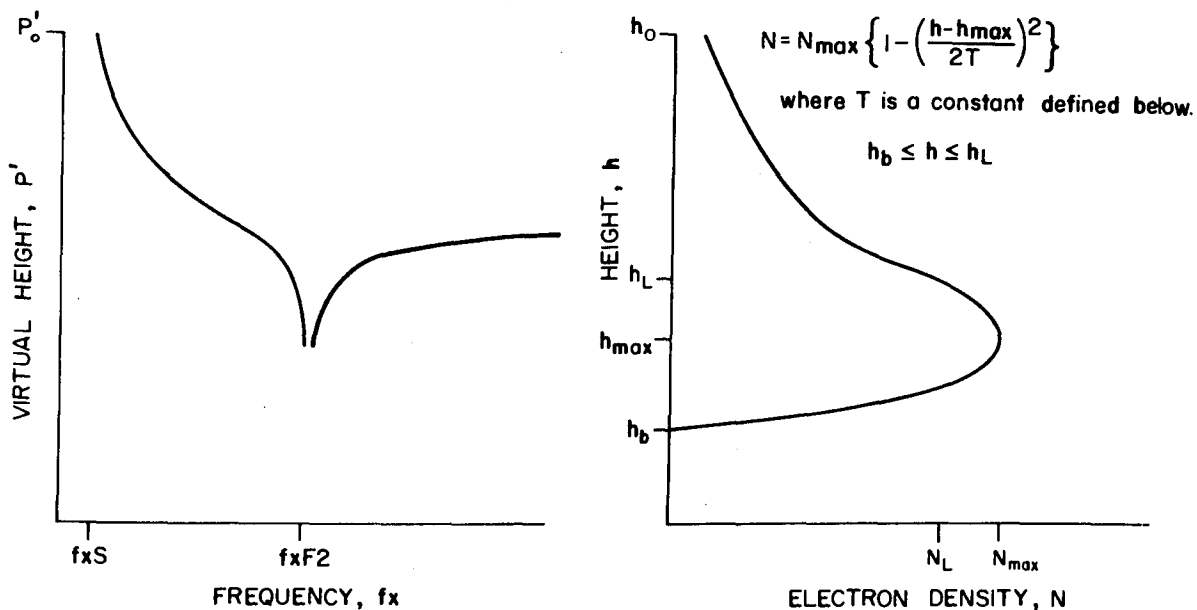


Figure 12. Ground Echoes Used for Estimation of Bottomside Total Electron Content

$$p'_m - p'_t = \int_{h_b}^{h_L} (\mu' - 1) dh + h_L, \quad (3.13)$$

where p'_m is the scaled group path (virtual height or apparent range);

p'_t is the group path from h_o to h_L ;

μ' is the group refractive index; a function of fx , gyrofrequency f_H , dip angle, and electron density, N .

The integral in (3.13) is transformed by

$$X = X_{\max} \left\{ 1 - \left[\frac{(h-h_{\max})}{2T} \right]^2 \right\} \quad (3.14)$$

where $X = (f_N/f_x)^2 = N/12400fx^2$

T = quarter thickness of the parabola to be determined.

This gives the single linear equation

$$R = T \left\{ \int_0^{X_{\max}} \frac{(\mu' - 1) dX}{X_{\max} \left(1 - \frac{X}{X_{\max}} \right)^{1/2}} + \int_{X_L}^{X_{\max}} \frac{(\mu' - 1) dX}{X_{\max} \left(1 - \frac{X}{X_{\max}} \right)^{1/2}} \right\} \quad (3.15)$$

where $R = p'_m - p'_t - h_L$.

The procedure adopted here, for the solution of (3.15) for T, is as follows:

- (1) A number, N_g , of pairs (p'_m, f_x) are scaled and smoothed. Only those pairs satisfying both
 - (a) $f_x F2 / f_x < 0.85$
 - (b) $p'_m - h_o > 60$ (km)
 are actually used in the calculation.
- (2) The $f_x F2$ (and $f_o F2$) are obtained from the ALOSYN data base.
- (3) The integral p'_t is computed using the original complete profiles of ALOUETTE $N(h)$, assuming μ' is linear in each height lamination.
- (4) The integrals on the right side of (3.15) are computed using the obvious trigonometric substitutions (to remove the singularity) followed by an application of the composite (closed) 5 point Newton-Cotes integration rule [24].
- (5) For each of the N_g pairs of scaled echoes determined in (1) above, there are a like number of linear equations:

$$R_i = TA_i \quad i = 1(1) N_g \quad (3.16)$$

where R_i and A_i are respective values of R and the integrals in (3.15). Equation (3.16) is solved for T by the method of least squares

$$\text{i.e. minimize} \quad \sum_{i=1}^{N_g} (R_i - TA_i)^2$$

Thus the parabola (3.14) on $[h_b, h_L]$ is completely determined, so that the method of section 3.2.2 may be used to determine an alternative version of slab thickness (h_{max} is found by making (3.14) continuous at (N_L, h_L)).

3.2.4 Illustration

In Tables 10(a)-(d) and 11(a)-(d), slab thickness has been displayed for various sets of input conditions. These values have been computed by the procedure outlined in section 3.2.2 and then sorted into a (crude) partition of the domain of the ALOSYN model, see below. The standard error, Se , of the mean slab thickness is given by

$$Se = S/N^{1/2} \quad (3.17)$$

where S = standard deviation of slab thickness,

N = ionogram count.

Also, the foF2 value displayed is a "check value" based on a peak electron density, Nmax, which is the ratio of the (average) TEC for the cell and the (average) slab thickness.

The data used in the preparation of these tables consisted of approximately 10,000 Alouette 1 profiles in the time period 1965-1970, or essentially half of the sunspot number cycle, Rz in [12, 112].

The domain was partitioned into 384 cells which consist of:

- (a) 2 longitude zones of 70° each, starting at 180°W
- (b) 3 geomagnetic latitude zones of 30° each, starting at 90°N
- (c) 2 magnetic activity zones, divided at Kp = 2.5 (between 2+ and 3-)
- (d) 2 sunspot number zones, divided at Rz = 40
- (e) 4 local time zones of 6 hours each, starting at midnight
- (f) 4 season zones of 3 months each, starting at January.

In Tables 10 and 11, only the results from the two most northern geomagnetic latitude zones, and for the eastern longitude zone, have been displayed -- these actually contained approximately 75% of the profiles used.

TABLE 10(a)

Mean and standard deviation of slab thickness (km), ratio of bottomside TEC to topside TEC, ionogram count and foF2 (MHz) for Latm $\geq 60^\circ$ N, Kp < 2.5, Rz < 40.

Local Time Month	[0,6]		[6,12]		[12,18]		[18,24]	
	January to March	232 .25	77 96	208 .23	70 108	219 .32	32 211	226 .34
	2.3		3.3		5.1		2.7	
April to June	215 .11	35 262	203 .12	30 435	248 .20	32 721	230 .21	33 327
	3.6		4.3		4.9		4.0	
July to September	*		-		-		-	
October to December	-		146 .09	23 4	-		-	
			5.7					

* No N(h) profiles available (in this sample).

TABLE 10(b)

Mean and standard deviation of slab thickness (km), ratio of bottomside TEC to topside TEC, ionogram count and foF2 (MHz) for Latm $\geq 60^\circ$ N, Kp > 2.5 , Rz < 40 .

Local Time Month	[0,6]	[6,12]	[12,18]	[18,24]
January to March	-	261 40 .39 4 3.7	211 15 .51 35 7.5	241 46 .32 144 2.9
April to June	287 27 .10 6 3.1	254 53 .15 45 4.7	298 48 .29 43 4.0	276 56 .27 88 3.6
July to September	-	-	-	-
October to December	-	-	-	-

TABLE 10(c)

Mean and standard deviation of slab thickness (km), ratio of bottomside TEC to topside TEC, ionogram count and foF2 (MHz) for Latm $\geq 60^\circ$ N, Kp < 2.5 , Rz > 40 .

Local Time Month	[0,6]	[6,12]	[12,18]	[18,24]
January to March	237 30 .48 58 3.3	-	323 42 .28 14 7.2	235 38 .59 29 4.7
April to June	250 25 .15 127 4.0	281 36 .16 234 4.2	285 27 .28 245 5.4	264 26 .40 5 6.5
July to September	-	269 14 .21 33 4.8	260 18 .27 22 5.9	-
October to December	-	186 45 .37 11 7.7	237 57 .51 21 7.0	240 26 .46 22 4.4

TABLE 10(d)

Mean and standard deviation of slab thickness (km), ratio of bottomside TEC to topside TEC, ionogram count and foF2 (MHz) for Lat_m ≥ 60° N, K_p > 2.5, R_z > 40.

Local Time Month	[0,6]		[6,12]		[12,18]		[18,24]	
January to March	313 .41 3.1	73 15	-	-	390 .42 5.1	16 9	361 .48 4.1	89 12
April to June	377 .34 3.2	100 21	280 .20 3.6	43 32	314 .29 4.6	41 95	-	-
July to September	315 .11 3.8	39 11	291 .17 4.0	27 51	305 .29 4.9	32 16	-	-
October to December	-	-	324 .28 6.8	7 10	220 .59 7.9	47 16	264 .39 4.7	77 40

TABLE 11(a)

Mean and standard deviation of slab thickness (km), ratio of bottomside TEC to topside TEC, ionogram count and foF2 (MHz) for Lat_m in [30° N, 60° N], K_p < 2.5, R_z < 40.

Local Time Month	[0,6]		[6,12]		[12,18]		[18,24]	
January to March	218 .40 3.5	41 151	187 .30 4.8	44 452	195 .31 5.7	26 204	248 .43 2.9	72 139
April to June	225 .41 2.7	57 322	179 .21 4.8	31 388	226 .53 6.0	35 590	223 .64 4.6	32 218
July to September	-	-	-	-	-	-	-	-
October to December	-	-	-	-	141 .20 5.6	4 4	-	-

TABLE 11(b)

Mean and standard deviation of slab thickness (km), ratio of bottomside TEC to topside TEC, ionogram count and foF2 (MHz) for Lattm in [30° N, 60° N], $K_p > 2.5$, $R_z < 40$.

Local Time Month	[0,6]	[6,12]	[12,18]	[18,24]
January to March	-	235 47 .29 73 4.4	199 47 .35 160 5.6	262 63 .66 55 2.9
April to June	259 51 .41 23 2.7	261 36 .28 29 4.4	243 27 .61 40 5.4	222 26 .73 61 4.0
July to September	-	-	-	-
October to December	-	-	-	-

TABLE 11(c)

Mean and standard deviation of slab thickness (km), ratio of bottomside TEC to topside TEC, ionogram count and foF2 (MHz) for Lattm in [30° N, 60° N], $K_p < 2.5$, $R_z > 40$.

Local Time Month	[0,6]	[6,12]	[12,18]	[18,24]
January to March	410 13 1.2 3 1.4	-	-	241 46 .66 15 7.6
April to June	228 35 .49 128 3.5	217 6 .14 4 3.9	248 24 .58 272 7.4	258 34 .61 27 6.9
July to September	-	409 36 .58 14 2.2	270 26 .45 38 5.1	-
October to December	-	201 49 .44 22 7.7	232 54 .59 21 7.2	228 4 .68 5 6.3

TABLE 11(d)

Mean and standard deviation of slab thickness (km), ratio of bottomside TEC to topside TEC, ionogram count and foF2 (MHz) for Lattm in [30° N, 60° N], Kp > 2.5, Rz > 40.

Local Time Month	[0,6]	[6,12]	[12,18]	[18,24]
January to March	393 34 .73 12 2.8	-	231 46 .48 19 8.9	-
April to June	298 108 .45 18 3.6	-	287 37 .77 33 8.5	-
July to September	-	306 35 .40 27 3.6	251 26 .47 22 7.0	-
October to December	-	266 41 .35 22 8.5	229 45 .64 44 7.8	269 30 .72 41 5.2

In Table 12, the results of computing slab thickness and the height of the base of the F2 layer have been compared for the two different parabolas used (with and without ground echoes). Of the 198 determinations made (or ionograms observed), from February 1965 and 1967, a systematic selection (every 18th determination) has been displayed.

The empirical model of slab thickness, Th, displayed in COMPUTER OUTPUT 3 is briefly described. The result of sorting the 10,000 ALOUETTE NH profiles into 384 cells yielded 132 points at which slab thickness is known:

$$(L_t_i, M_i, Lattm_i, Kp_i, Long_i, Rz_i, Th_i), i = 1(1)132$$

The majority of these points occurred in the two most northeast geographic zones since that was where the majority of the 10,000 profiles occurred. The 252 = (384 - 132) empty cells correspond to non-existent keyed records on the file THICK, (see also Appendix A).

These points were then fitted to a model of the form:

TABLE 12

Comparison of Slab Thickness Without Ground Echoes (Section 3.2.2) and with Ground Echoes (Section 3.2.3)

WITHOUT GROUND ECHOES		WITH GROUND ECHOES	
HEIGHT OF BASE OF LAYER, h_b (km)	SLAB THICKNESS (km)	HEIGHT OF BASE OF LAYER, h_b (km)	SLAB THICKNESS (km)
199	208	135	252
211	239	145	281
227	188	126	252
193	190	155	210
207	350	137	400
210	318	235	246
216	360	170	391
217	265	156	306
199	174	158	203
221	198	261	170
226	168	223	129
236	260	-126	514

$$\begin{aligned}
 Th(x_1, x_2, x_3, x_4, x_5, x_6) = & b_0 + \sum_{j=1}^4 b_{2j-1} \sin^j x_1 + b_{2j} \cos^j x_1 \\
 & + \sum_{j=1}^2 b_{2j+7} \sin^j x_2 + b_{2j+8} \cos^j x_2 \\
 & + \sum_{j=1}^4 b_{j+12} x_3^j + \sum_{j=1}^4 b_{j+16} x_4^j \\
 & + \sum_{j=1}^2 b_{j+20} x_5^j + \sum_{j=1}^2 b_{j+22} x_6^j
 \end{aligned} \tag{3.18}$$

The actual 6 independent variables used were:

$$\begin{aligned}
 x_1 &= \pi Lt/12 && Lt \text{ in } [0,24] \\
 x_2 &= \pi(2M-1)/12 && M \text{ in } [.5,12.5] \\
 &&& \text{(integer months denote mid-months)} \\
 x_3 &= Lattm/90 && Lattm \text{ in } [0,90] \\
 x_4 &= Kp/9.3 && Kp \text{ in } [0,9] \\
 x_5 &= (Long + 180)/140 && Long \text{ in } [-180^\circ, -40^\circ] \\
 x_6 &= Rz/120 && Rz \text{ in } [0,150]
 \end{aligned}$$

The statistically significant coefficients, b_j : $j=0(1)24$, were computed by the subroutines STEP1 and STEP2. In this case, the actual coefficients were:

$$\begin{aligned}
 b_0 &= 166.05 & b_1 &= -38.462 & b_3 &= 32.407 \\
 b_5 &= 63.112 & b_9 &= 7.9556 & b_{10} &= -29.452 \\
 b_{16} &= 57.693 & b_{17} &= 100.47 & b_{24} &= 119.29
 \end{aligned}$$

and the root mean square error for the errors in predicted thickness was 34 km. As a matter of interest, all the variables except longitude appeared in the model (3.18).

The subroutine SLABTH in the main prediction program PREDSYS actually computes slab thickness for the user-specified conditions and for each hour of local time.

In conclusion, the following remarks pertaining to these illustrations are made:

- (a) More profile data is needed to cover the entire sunspot range adequately. These data exist (see ISIS 1 and 2, Table 8) where one observes that there are approximately 70,000 more profiles, in the North American sector, which may be used. These, combined with the early Alouette 1 profiles would give a fairly extensive data base of approximately 130,000 ionograms (= 50,000 + 10,000 + 70,000). While this is still only about one third of the size of the ALOSYN data base used, it would permit a finer cell division (than used in Tables 10 - 11) and also fill in some of the seasonal gaps observed in the latter.
- (b) Even with an extended data base, there still exists the uncertainty of determining the profile (and TEC) on the bottomside of the F2 layer, from topside data only. While it may not be feasible to use the "ground echo" approach everywhere (recall reasons in section 3.2.2), there do exist extensive bottomside synoptic data (scaled and recorded on magnetic tape) containing ionospheric

characteristics such as foF2, foF1, foE, h'F2, h'F, M(3000)F2, and M(3000)F1 for ground stations located at Resolute, Churchill, Winnipeg-Kenora, Ottawa, and St. John's, at least. (See Tapes 5E08, 4B32, and 4B33 in Appendix A). These data would certainly give at least a "representative" parabola, or combination of parabolas, for the bottomside profile, using the classical Abel equation (see [8] of Bibliography) relating scaled ionograms and electron density profiles.

4. MAIN TROUGH REFINEMENTS

4.1 DESCRIPTION OF THE PROCEDURE

Beginning with Muldrew [17], extreme troughs have been consistently observed in the spatial electron density, particularly in the sunset to sunrise period of the day and at mid and high geomagnetic latitudes. In addition, regular movements of the trough have been observed (equatorward with increasing magnetic activity and local time tending towards midnight). Tulunay and Sayers [28], using data from the Ariel III satellite launched in 1967, compiled a statistical summary of trough crossings over an 11 month period. In particular, they noted that most of the troughs were observed in the geomagnetic latitude range [50°N, 70°N]. In Pike [22], there is a set of linear equations for predicting foF2 from a "reference latitude coordinate system". These are for a very limited period of time (December 1971 ISIS 2 data). Halcrow and Nisbet [10] produced a trough model using 30,000 profiles of Alouette 1 and 2 in the time period 1962-70. The output from their model was a multiplicative factor, depending on invariant latitude, Kp, Lt, and Rz which could be applied to the Nmax (or foF2) as predicted by the C.C.I.R. model, [5]. Essentially they defined it as unity at the north and south edges of the trough and 0.25 at the centre, for Nmax.

The procedure adopted here is essentially to use the ALOSYN model to locate the trough for a given longitude, month, local time, sunspot number, and magnetic activity. The changes in foF2 between the trough edges and the centre will then be modified to agree with Halcrow and Nisbet's observations to partially account for the smoothing that has occurred due to the averaging of ionogram parameters in the cells.

More precisely, the procedure is as follows:

- (1) The ALOSYN model is used to generate an array of points ($Lattm_k$, $foF2_k$) in $[45^\circ, 75^\circ]$ (geomagnetic), $k = 1(1)13$, for a given longitude, local time, Kp, month and Rz. The model actually gives pairs at every 5 degrees of latitude - additional interpolants have been filled in using a cubic spline technique.
- (2) Locate the trough centre, M; i.e. that point ($Lattm_M$, $foF2_M$) where foF2 takes its absolute minimum in $[45^\circ, 75^\circ]$.
- (3) The north and south edges, N and S respectively, are taken to be the nearest points of inflection about the centre M, i.e. ($Lattm_N$,

$foF2_N$) and $(Lattm_S, foF2_S)$ respectively. This is the reason why interpolants were generated above; recall that the trough is about 5 degrees wide (north to south). See also [10,17,19].

(4) Finally, the corrected $foF2$ at the centre is defined by:

$$foF2_{C(M)} = \max [\frac{1}{2} \min(foF2_N, foF2_S), foF2\%] \quad (4.1)$$

where $foF2\%$ is a 5-percentile which is also obtainable from the ALOSYN model. The 5-percentile of $foF2$ is taken from the distribution of $foF2$ at the point $(lattm_M, foF2_M)$. An example of an averaged and corrected trough is now presented.

4.2 ILLUSTRATION

In Figures 13(a)-(d), profiles of $foF2$ against latitude have been displayed for the indicated conditions (January - March, 1963 has an R_z of approximately 29). Unstandardized (1963) data have been used in these plots.

All the plots are for the eastern-most longitude zone $[-90^\circ, -45^\circ]$. For a given figure, the 4 profiles represent the 4 local time zones for the month. For each curve the local time can range up to 5 to 6 hours over the

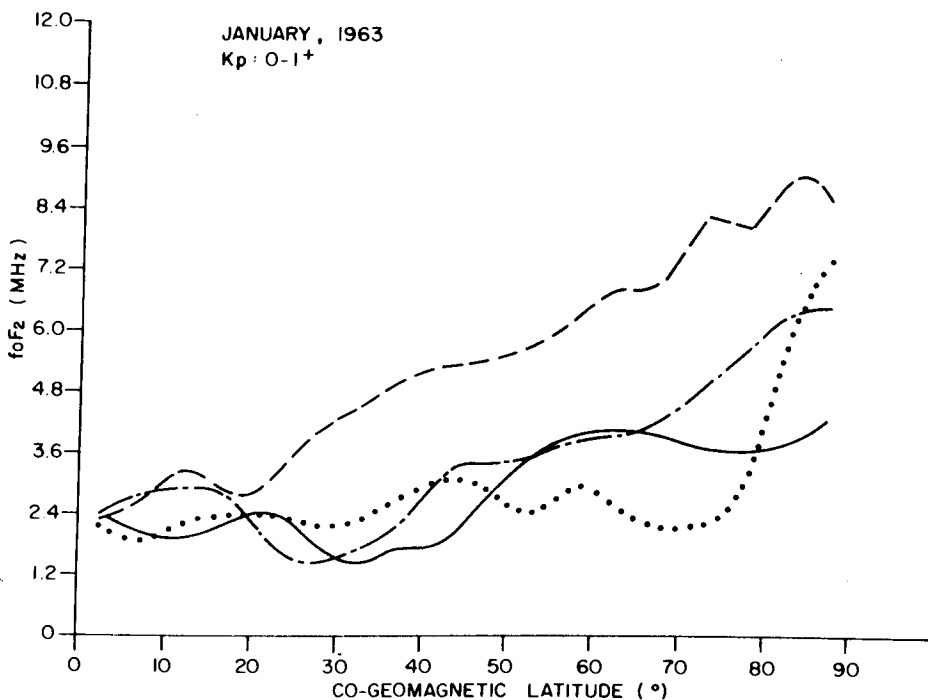


Figure 13(a). Illustration of the main trough for low sunspot number, longitude in $[90^\circ W, 45^\circ W]$ and local time in Table 13, January, 1963, $K_p < 1.5$.

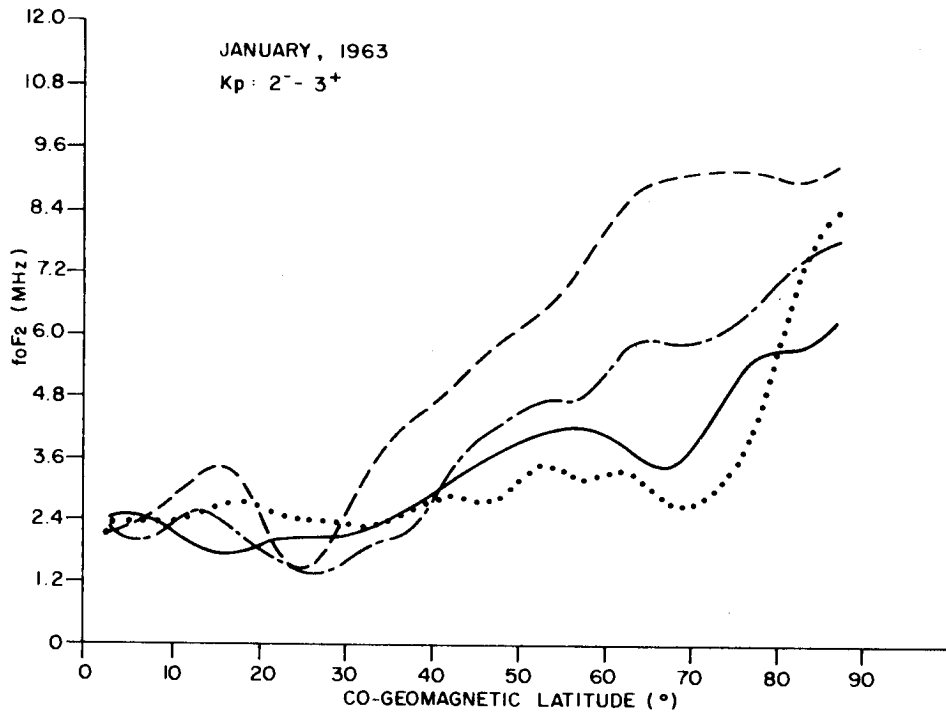


Figure 13(b). Illustration of the main trough for low sunspot number, longitude in $[90^{\circ}W, 45^{\circ}W]$ and local time in Table 13, January, 1963, $1.5 < Kp < 3.5$.

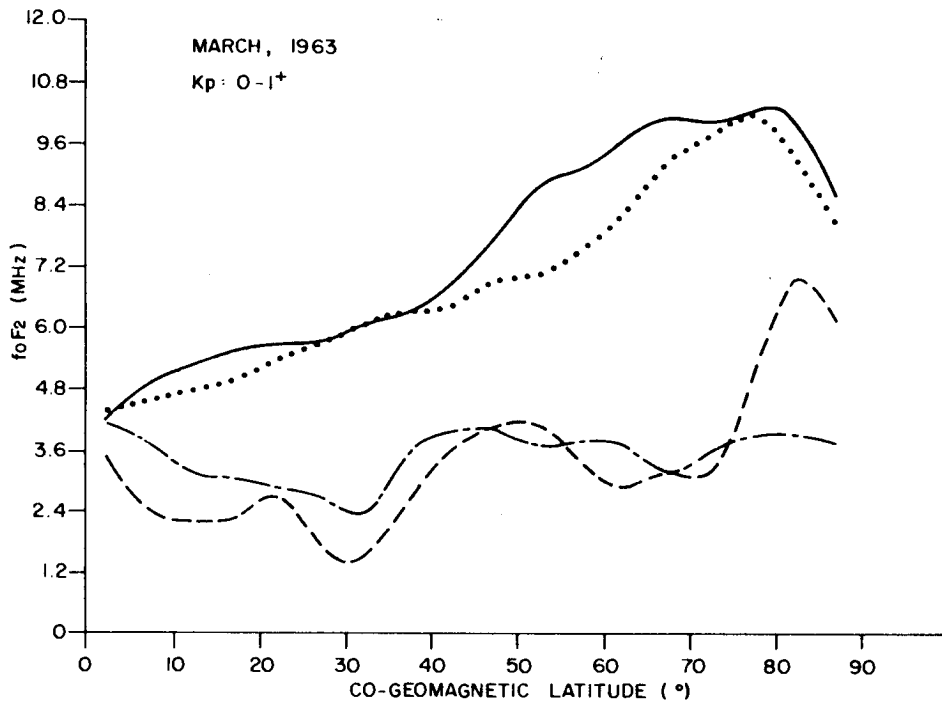


Figure 13(c). Illustration of the main trough for low sunspot number, longitude in $[90^{\circ}W, 45^{\circ}W]$ and local time in Table 13, March, 1963, $Kp < 1.5$.

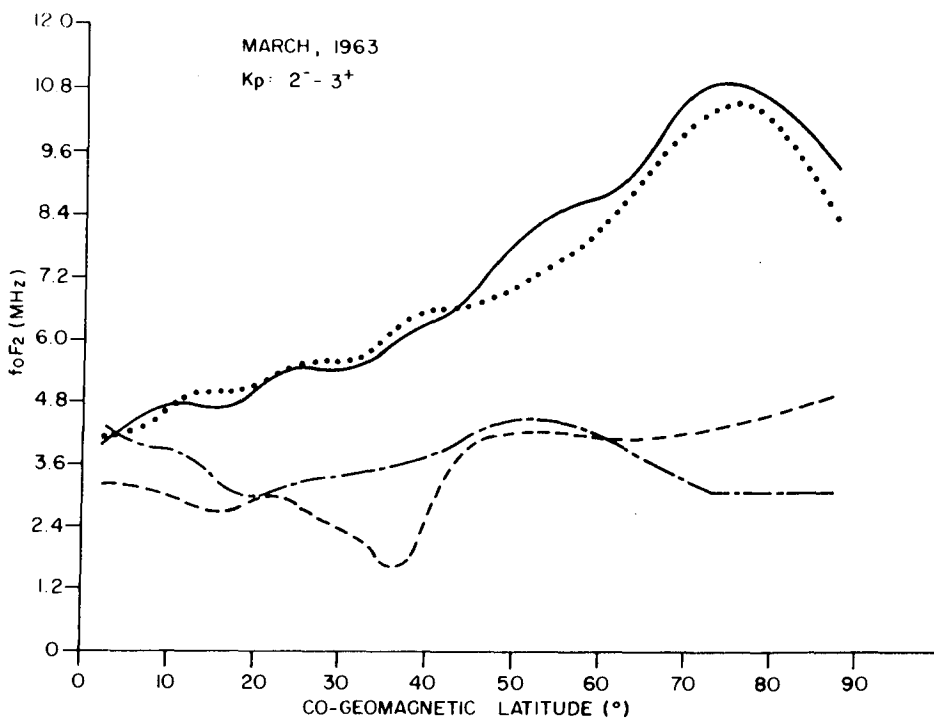


Figure 13(d). Illustration of the main trough for low sunspot number, longitude in $[90^{\circ}W, 45^{\circ}W]$ and local time in Table 13, March, 1963, $1.5 < K_p < 3.5$.

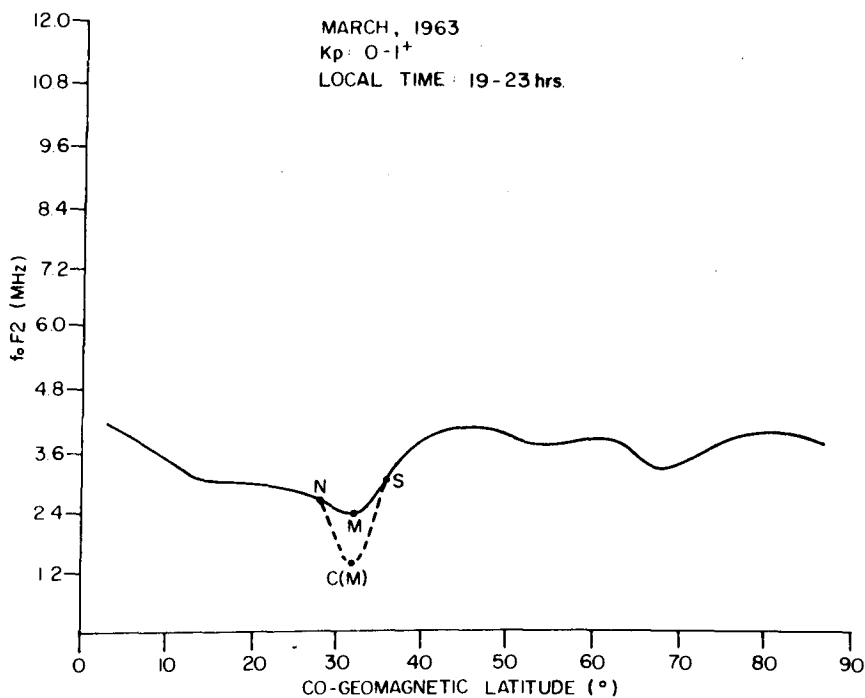


Figure 13(e). An example of the trough correction procedure for low sunspot number, longitude in $[90^{\circ}W, 45^{\circ}W]$.

entire latitude range. For convenience, these local time ranges are given in Table 13. Some evidence of a trough (near a co-geomagnetic latitude of 30°) appears in all the figures except the March 1963 midday curves.

In Figure 13(e), the trough correction procedure is illustrated for the March low magnetic activity trough which appears to begin to form at about 19 to 23 hours local time. (One should observe also Figure 13(c) and note that this trough has become more accentuated at approximately 21 to 2 hours, local time. The actual step by step trough correction is now illustrated. In the neighbourhood of the trough the following interpolants have been generated:

k	Lattm	foF2	foF2%
1	75.0	3.0	
2	72.5	3.0	1.7
3	70.0	2.9	
4	67.5	2.8	1.7
5	65.0	2.7	
6 N	62.5	2.6	1.9
7	60.0	2.3	
8 M	57.5	2.3	1.1
9	55.0	2.8	
10 S	52.5	3.5	2.9
11	50.0	3.8	
12	47.5	3.9	2.4
13	45.0	3.9	

as well as a 5% - tile of foF2, from the actual cell histograms. The pairs used for the north and south edge as well as the centre have also been appropriately labelled. Thus the corrected foF2 at the centre becomes, using (4.1):

$$\text{foF2} = \max \left[\frac{1}{2} \min(2.6, 3.5), 1.1 \right] = 1.3 \text{ MHz}$$

The centre is still assumed to be located at Lattm = 57.5°N .

In conclusion, the prediction system (PREDSYS and associated XEQ file, i.e. execute file in Honeywell CP-V system, EXPREDSYS) has been set up so as to allow the user to optionally make trough corrections, by hand, using the above illustration as a guide. In other words, after one has made sets of predictions for several latitudes (at most 19), a file will exist containing grids of the characteristics (foF2, spread, and slab thickness in local time

TABLE 13

Local time code for Figures 13(a) to 13(e)

LOCAL TIME CELL INDICES (LT1,LT2)	GRAPHIC SYMBOL	LOCAL TIME RANGE (Hours) (ALL LATITUDES)	
		JANUARY	MARCH
(1,1)	_____	[21,2]	[13,18]
(1,2)	-----	[5,10]	[21,2]
(2,1)	[19,24]	[11,16]
(2,2)	-----	[3,7]	[19,23]

and latitude). The user is then permitted to edit this file (using the EDIT processor of the Honeywell Sigma 9 computer) in order to make trough corrections, fill in "missing values" resulting from the lack of cells in ALLMON, and even correct "obvious" bad predictions. To aid in this, the user may access those cells that are available (see COMPUTER OUTPUT 4), and also access files of preliminary interpolates (see section 2.3.2), which are also produced by the prediction system at the user's option.

Upon completion of this editing task, the user may resume use of the XEQ file EXPREDSYS, to display the contour maps.

5. ACKNOWLEDGEMENT

Most of the work was done while the author was a Visiting Fellow at CRC under the sponsorship of the Department of National Defense. The author also acknowledges the support of D.B. Muldrew for his assistance and guidance.

6. REFERENCES

1. *Alouette 1 Ionospheric Data, ALOSYN*, Defence Research Board Telecommunications Establishment (now Communications Research Centre, Department of Communications), Ottawa, Canada, 1970.
2. *Alouette 1 Ionospheric Data N(h)*, Defence Research Board Telecommunications Establishment (now Communications Research Centre, Department of Communications), Ottawa, Canada, 1970.
3. *Alouette 1 (1962 Beta Alpha 1) Topside Sounder (Data Users' Note)*, National Space Science Data Center, Report No. 67-29, National Aeronautics and Space Administration, Goddard Space Flight Center, Greenbelt, Md., 1967.
4. Calvert, W., and C.W. Schmid, *Spread-F Observations by the Alouette Topside Sounder Satellite*, J. Geophys. Res., 69, 1839-1852, 1964.
5. *C.C.I.R. Atlas of Ionospheric Characteristics*, Report 340, Geneva, 1967.
6. Davies, K., *Ionospheric Prediction and Extrapolation*, Proceedings of the Advisory Group for Aerospace Research and Development, N.A.T.O., Ottawa, Canada, 1978.
7. Dyson, P.L., *A Method for Determining the Electron Density Distribution about the F₂ Peak of the Ionosphere*, Aust. J. Phys., 25, 293-297, 1972.
8. Fraser, D.A.S., *Statistics an Introduction*, Wiley, New York, 1958.
9. Hagg, E.L., Hewens, E.J., and G.L. Nelms, *The Interpretation of Topside Sounder Ionograms*, Proc. IEEE., 57, 949-960, 1969.
10. Halcrow, B.W., and J.S. Nisbet, *A Model of F₂ Peak Electron Densities in the Main Trough Region of the Ionosphere*, Radio Sci., 12, 815-820, 1977.
11. Jackson, J.E., *The Reduction of Topside Ionograms to Electron - Density Profiles*, Proc. IEEE., 57, 960-976, 1969.
12. Jackson, J.E., *Comparisons Between Topside and Ground - Based Soundings*, Proc. IEEE., 57, 976-985, 1969.
13. Jones, W.B., and R.M. Gallet, *The Representation of Diurnal and Geographic Variations of Ionospheric Data by Numerical Methods*, I.T.U. Telecommunications Journal, 29, 129-147, 1960.
14. Kohnlein, W., *Electron Density Models of the Ionosphere*, Rev. Geophys. Space Phys., 16, 341-354, 1978.
15. Llewellyn, S.K., and R.B. Bent, *Documentation and Description of the Bent Ionospheric Model*, Air Force Cambridge Research Laboratories, Space and Missile System Organization, Los Angeles, California, 1973.

16. Mendillo, M., and M. Buonsanto, *The Ionospheric F-Region Near 60° Magnetic Latitude: Monthly Mean Behavior and Substorm Effects During Winter Nights*, Annual Scientific Report No. 2, Department of Astronomy, Boston University, Boston, Mass., 1976.
17. Muldrew, D.B., *F-Layer Ionization Troughs Deduced from Alouette Data*, J. Geophys. Res., 70, 2635-2650, 1965.
18. Muldrew, D.B., Gladwin, C.J. and H.G. James, *An F-Layer Model for North America and its Application to the Search and Rescue Satellite Program*, Proc. of Symposium on Beacon Satellite Measurements of the Plasmaspheric and Ionospheric Properties, Florence, Italy, 1978.
19. Muldrew, D.B., and H.G. James, *Ionospheric Effects on the Doppler Frequency Shift in Sarsat Propagation*, CRC Report 1313, Communications Research Centre, Department of Communications, Ottawa, Canada, 1978.
20. Petrie, L.E., *High-Frequency Propagation Predictions using an IBM 650 Computer*, Report No. 1117, Defence Research Telecommunications Establishment, Ottawa, 1963.
21. Petrie, L.E., and G.E.K. Lockwood, *On the Prediction of F-Layer Penetration Frequencies*, Proc IEEE., 57, 1025-1028, 1969.
22. Pike, C.P., *An Analytical Model of the Main F-layer Trough*, Report AFGL-TR-76-0098, Air Force Geophysics Laboratory (Ionospheric Physics Division), Hanscom AFB, Mass., 1976.
23. *Prediction of Optimum Traffic Frequencies for Northern Latitudes*, Parts I and II, DRTE/RPL Report No. 1-1-3, Ottawa, 1954.
24. Ralston, A., and H.S. Wilks, *Mathematical Methods for Digital Computers*, Wiley, New York, 1959.
25. Rosich, R.K., and W.B. Jones, *The Numerical Representation of the Critical Frequency of the F1 Region of the Ionosphere*, Report No. 73-22, Office of Telecommun., U.S. Dep. of Commer., Boulder, Col., 1973.
26. Schmid, P.E., Bent, R.B., Llewellyn, S.K., Nesterczuk, G., and S. Rangaswamy, *NASA-GSFC Ionospheric Corrections to Satellite Tracking Data*, Report X-591-73-281 Goddard Space Flight Centre, Greenbelt, Md., 1973.
27. Shimazaki, T., *World-wide Daily Variation in the Height of the Maximum Electron Density of the Ionospheric F2 Layer*, J. Radio Res. Labs. Japan, 2, 85, 1955.
28. Tulunay, Y., and J. Sayers, *Characteristics of the Mid-latitude Trough as Determined by the Electron Density Experiment on Ariel III*, J. of Atmos. Terr. Phys., 33, 1737-1761, 1971.

7. BIBLIOGRAPHY

Additional material concerning ionospheric modelling is presented here.

1. Aarons, J., Buchau, J., Mullen, J.P., Weber, E.J., Whalen, J., and H.E. Whitney, *Ground and Airborne Scintillation Studies of AFSATCOM DT&E/IOT&L*, AFGL-TR-76-0164, Air Force Geophysics Laboratory (PH) Hanscom AFB, Mass., 1976.
2. Aarons, J., and R.S. Allen, *Scintillation Boundary During Quiet and Disturbed Magnetic Conditions*, *J. Geophys. Res.*, 76(1), 170-177, 1971.
3. Aarons, J., Mullen, J., and S. Basu, *The Statistics of Satellite Scintillations at a Subauroral Latitude*, *J. Geophys. Res.*, 69(9), 1785-1794, 1964.
4. Donatelli, D.E., Hartmann, G.K., R., Leitinger, and Allen, R.S., *Adaptive Mapping of Mid-Latitude Ionosphere*, Report AFGL-TR-77-0176, Air Force Geophysics Laboratory (PHP), Hanscom AFB, Mass., 1977.
5. Arendt, P.R., *Comparison of Columnar Ionospheric Electron Content Obtained from Simultaneous Measurements of Faraday Rotation and Doppler Shift*, Report ECOM-3170 Electromagnetic Transmission Research Area, Fort Monmouth, N.J., 1969.
6. Bent, R.B., Llewellyn, S.K., Nesterczuk, G., and P.E. Schmid, *The Development of a Highly-Successful Worldwide Empirical Ionospheric Model and its Use in Certain Aspects of Space Communications*, J.M. Goodman, Editor, Based on Ionospheric Effects Symposium, Crystal City, Arlington Va., January, 1975, USGPO Stock Number 008-051-00064-0, 13-28.
7. Buchau, J., Pike, C.P., and M. Wong, *Detailed Specification of the Arctic Ionosphere and an Application to Three-Dimensional Raytracing*, Report No. AFCRL-TR-73-0726, Air Force Cambridge Research Laboratories, Hanscom AFB, Mass., 1973.
8. Budden, K.G., *Radio Waves in the Ionosphere*, Cambridge University Press, 1961.
9. Burke, W.J., Donatelli, D.E., Sagalyn, R.C., and M.C. Kelley, *Low Density Regions Observed at High Altitudes and their Connection with Equatorial Spread F*, *Planet. Space Sci.*, 27, 593-601, 1979.
10. Chan, K.L. and L. Colin, *Global Electron Density Distributions from Topside Soundings*, *Proc. IEEE.*, 57(6), 990-1005, 1969.
11. Clemesha, B.R., and R.W.H. Wright, *A Survey of Equatorial Spread F, Spread F and its Effects Upon Radiowave Propagation and Communications*, P. Newman, Editor, The Advisory Group for Aerospace Research and Development, NATO, Technivision, Maidenhead, England, 1966.

12. DuCharme, E.D., and L.E. Petrie, *A Method for Predicting the F1 Layer Critical Frequency Based on the Zurich Smoothed Sunspot Number*, Radio Sci., 8(10), 837-839, 1973.
13. Eccles, D., and J.W. King, *A Review of Topside Sounder Studies of the Equatorial Ionosphere*, Proc. IEEE., 57(6), 1012-1019, 1969.
14. Flattery, T.W., and A.C. Ramsay, *Derivation of the Total Electron Content for Real Time Global Applications, Effects of the Ionosphere on Space Systems and Communications*, J.M. Goodman, Editor, Based on Ionospheric Effects Symposium, Crystal City, Arlington Va., January 1975, USGPO Stock Number 008-051-00064-0, 336-344.
15. Fremouw, E.J., and C.L. Rino, *An Empirical Model for Average F-Layer Scintillation at VHF/UHF*, Radio Sci., 8(3), 213-222, 1973.
16. Gassmann, G.J., Buchau, J., Wagner, R.A., Pike, C.P. and M.G. Hurwitz, *Arctic Ionospheric Modelling-Five Related Papers*, AFCRL 72-0305, Air Force Cambridge Research Laboratories, Hanscom AFB, Mass., 1972.
17. Goldberg, R.A., *A Review of the Theories Concerning the Equatorial F2 Region Ionosphere*, Proc. IEEE., 57(6), 1119-1126, 1969.
18. Goutelard, C., and J. Caratori, *Modelisation de l'Ionosphere dans les Problemes de Gestion de Reseaux de Transmission HF*, AGARD Conference Proceedings No. 238 (Volume 1), Operational Modelling of the Aerospace Propagation Environment, H. Soicher, Editor, Ottawa, April. 1978.
19. Jelly, D.H., and L.E. Petrie, *The High-latitude Ionosphere*, Proc. IEEE., 57(6), 1005-1012, 1969.
20. Johanson, J.M., Buonsanto, M.J., and J.A. Klobuchar, *The Variability of Ionospheric Time Delay*, Proceedings of the Symposium on the Effect of the Ionosphere on Space and Terrestrial Systems, sponsored by Naval Research Laboratory and the Office of Naval Research, Washington, D.C., January, 1978.
21. Jones, W.B., and R.M. Gallet, *Methods for Applying Numerical Maps of Ionospheric Characteristics*, Journal of Research NBS 66D (Radio Propagation), 6, 649-662, 1962.
22. Jones, W.B., and R.M. Gallet, *Representation of Diurnal and Geographic Variations of Ionospheric Data by Numerical Methods*, I.T.U. Telecommunication Journal, 32, 1, 18-28, 1965.
23. Klobuchar, J.A., and J.M. Johanson, *Correlation Distance of Mean Daytime Electron Content*, Report AFGL-TR-77-0185, Air Force Geophysics Laboratory (PHP), Hanscom AFB, Mass., 1977.
24. McNamara, L.F., *Model Starting Height for N(h) Analyses of Ionograms*, Atmos. and Terr. Phys., 40, 543-547, 1979.

25. Nelms, G.L., *Seasonal and Diurnal Variations of the Distribution of Electron Density in the Topside of the Ionosphere*, Electron Density Profiles in the Ionosphere and Exosphere, Jon Frihagen, Editor, Proceedings of the NATO Advanced Study Institute, Finse, Norway, April, 1965.
26. Nisbet, J.S., *Operational Physical Models of the Ionosphere*, AGARD Conference Proceedings No. 238 (Volume 1), Operational Modelling of the Aerospace Propagation Environment, H. Soicher, Editor, Ottawa, April, 1978.
27. Norton, R.B., *The Middle-Latitude F Region During Some Severe Ionospheric Storms*, Proc. IEEE., 57(6), 1147-1150, 1969.
28. Olson, W.P., and K.A. Pfitzer, *A Quantitative Model of Ionospheric Electron Density*, Report MDC G7433 McDonnell Douglas Astronautics Company, Huntington Beach, Ca., 1978.
29. Petrie, L.E., *Preliminary Results on Mid and High Latitude Topside Spread F, Spread F and its Effects upon Radiowave Propagation and Communication*, P. Newman, Editor, The Advisory Group for Aerospace Research and Development, NATO, Technivision, Maidenhead, England, 1966.
30. Pike, C.P., *A Comparison of the North - and South - Polar F Layers*, J. Geophys. Res., 76(28), 6875-6881, 1971.
31. Pike, C.P., *A Latitudinal Survey of the Daytime Polar F Layer*, J. Geophys. Res., 76(31), 7745-7753, 1971.
32. Rawer, K., Bilitza, D., and S. Ramakrishan, *Goals and Status of the International Reference Ionosphere*, Rev. of Geophys. Space Phys., 16(2), 177-181, 1979.
33. Rawer, K., *The Ionosphere*, Ungar, New York, 1956.
34. Rush, C.M., *An Ionospheric Observation Network for use in Short-term Propagation Predictions*, I.T.U. Telecommunication Journal, 43, 544-549, 1976.
35. Rush, C.M., and D. Miller, *A Three-dimensional Ionospheric Model using Observed Ionospheric Parameters*, Report AFCRL-TR-73-0567, Air Force Cambridge Research Laboratories (LII), Hanscom AFB, Mass., 1973.
36. Rush, C.M., *Ionospheric Predictions: Methods and Results*, AGARD Conference Proceedings No. 238 (Volume 1), Operational Modelling of the Aerospace Propagation Environment, H. Soicher, Editor, Ottawa, April, 1978.
37. Rush, C.M., and W.R. Edwards, Jr., *Sensitivity of HF Circuit Simulations to Electron Density Models*, Radio Sci., 10(10), 867-874, 1975.
38. Shirke, J.S., and S.S. Degaonkar, *Origin of Annual and Subannual Periodicities in F Region Ionization*, J. Geophys. Res. 83(A3), 983-988, 1978.

39. Thomas, J.O., Briggs, B.R., Colin, L., Rycroft, M.J., and M. Covert, *Ionosphere Topside Sounder Studies, 1 - The Reduction of Alouette 1 Ionograms to Electron Density Profiles*, Report TN D-2882, NASA, July, 1965.
40. Thompson, R.L., *User Requirements of Aerospace Propagation-Environment Modelling and Forecasting*, AGARD Conference Proceedings, No. 238 (Volume 1), Operational Modelling of the Aerospace Propagation Environment, H. Soicher, Editor, Ottawa, April, 1978.
41. Titheridge, J.E., *Exospheric Temperature and Composition from Alouette 1 Electron Density Profiles*, Report 74/1, Radio Research Centre, University of Auckland, New Zealand, 1974.
42. *URSI Handbook of Ionogram Interpretation and Reduction*, W.R. Piggott and K. Rawer, Editors, Elsevier, Amsterdam, 1961.
43. Wagner, R.A., Snyder, A.L., and S.I. Akasof, *The Polar Ionosphere During Exceptionally Quiet Periods*, Planet. Space Sci., 21, 1911-1922, 1973.
44. Warren, E.S., *The Topside Ionosphere During Geomagnetic Storms*, Proc. IEEE., 57(6), 1029-1036, 1969.
45. Whitney, H., Aarons, J., Allen, R.S., and D.R. Seemann, *Estimation of the Cumulative Amplitude Probability Distribution Function of Ionospheric Scintillations*, Radio Sci., 7(12), 1095-1104, 1972.
46. Wright, J.W., Van Zandt, T.E., and G.H. Stonehocker, *Data on Ionospheric Electron Densities - I, Tables and Isoionic Maps for Selected Times in October 1957*, National Bureau of Standards Report 5590, Boulder, Colorado, 1958.

APPENDIX A

Glossary of Files and Tapes

In this Appendix, the files associated with each section of the report are listed (in application order) and briefly described. Each such description is prefixed by the code:

FILENAME, TYPE, ORG.

where (1) FILENAME is the name of file

(2) TYPE is one of the letters X,B,F, or D corresponding to XEQ, BATCH, FORTRAN source, or data files.

(3) ORG is one of K3, K11, or C describing the key structure of the file. Here K3 denotes files with 3 byte (EDIT) keys, K11 with 11 byte (direct access) keys, and C for sequential files (no keys)..

Any F file is compiled on the file BFILENAME in single precision, unless the contrary is stated.

Any compiled version of an F file is loaded with LYNX and the file BMISC, unless the contrary is stated.

In some cases, for a related set of a files, two numbers denoted by XX will be suffixed to the file name and will be defined at that point.

The file, EXFILENAME, will denote an X file for the associated F file, FILENAME. The source listings of all X,B and F files are available on request. See Tape 5E47 below.

The first file is of general purpose and applies to the entire report.

MISC,F,K3.

All miscellaneous, non-standard subroutines not displayed explicitly elsewhere are here. It should be compiled with the batch compile (BC) option.

Section 2.2.1

CRALOMON,X,K3.

This file controls the transfer of the original ALOSYN tapes to disk.

DXX,D,K3. XX = 62(1)68

These 7 files are built by the user in CRALOMON. Each contains 1 record with 2 integers which are used for positioning an ALOSYN tape to the month to be processed. See also IONMODELS.

DMON,D,K3.

This file is built in CRALOMON and consists of 1 record with 8 integers to be used for defining the cell alignment. See also IONMODELA.

ALOMONXX,D,C. XX = 62(1)68

These 7 files each consist of the same month of ALOSYN data, for each year XX.

CXX,D,C. XX = 62(1)68

Each of these files contain 5 records with certain quality statistics concerning the respective ALOMONXX. See also IONMODELS.

IONMODELS,F,K3.

This program produces ALOMONXX and CXX, one year at a time.

DUMFILE,-,K3.

Records 9 to 28 are PCL commands used for removing and accessing ALOSYN tapes as they are processed.

CNSTRPCL,F,K3.

This is used for copying the last 3 records of ALOMONXX. The actual number of records of ALOMONXX is given by the first record of the appropriate CXX. It should be compiled with the BC option.

AXX,B,K3. XX = 62(1)68

These 7 files control the production of DUMXX, respectively. They are "batched" by CRALOMON.

BXX,B,K3. XX = 62(1)68

These 7 files control the production of MONXX, respectively. They are "batched" by CRALOMON.

Section 2.2.2

DUMXX,D,C. XX = 62(1)68

These 7 files contain the cell indices, input averages, and extreme foF2 values for the ionograms of ALOMONXX.

IONMODELA,F,K3

This produces DUMXX from ALOMONXX, one year at a time.

MONXX,D,C. XX = 62(1)68

These 7 files are the respective DUMXX updated with the histograms of foF2 and spread F.

IONMODELB,F,K3.

This produces MONXX given an ALOMONXX and a DUMXX.

REDUALO,F,K3.

The orbital position parameters of the satellite are corrected on ALOMONXX using this program. (see February, 1965).

IONGACC,F,K3.

Individual ionograms from user specified cells are accessed from ALOMONXX.

SATTRACK,F,K3.

This creates a file of orbital position parameters of the satellite, for a given time interval. These data are used in the construction of Figure 4. See also EXSATTRACK.

Section 2.2.3

MERMON,X,K3.

This controls the merging and blocking of the MONXX files, as well as the production of ALLMON.

DUMFILE,-,K3.

Records 2 to 8 contain merging and blocking specification parameters required by the system MERGE processor. Record 1 contains two integers which are required as input for IONMODEL C.

MON,D,C

The merged version of all the MONXX files.

MONB96,D,C.

The blocked version of MON. Nyear years for a given cell are blocked together on a record (in increasing year order). Each record has 96*Nyear bytes. All empty cells are included, in order to facilitate the accession of user-specified cells. These files, all months, have been stored on magnetic tape. See tape listing below.

ZR6278,D,K3.

This consists of 34 records; the odd records are the monthly Zurich sunspot numbers for each year of 1962-78, while the even records are the smoothed monthly Zurich sunspot numbers.

YEAR,D,K3.

This contains one record with two integers specifying the month and the number of years to be processed by IONMODEL C. See also record 1 of DUMFILE.

IONMODEL C,F,K3.

This standardizes the records of MONB96 to the average sunspot number of the cell.

MONSTD,D,K11.

A keyed file corresponding to the standardized month represented by MONB96 and produced by IONMODEL C. Only those cells to be used in interpolation are kept.

ALLMON,D,K11.

The concatenated version of MONSTD for all months. The maximum allowable key is FFFFFFFF₁₆ or 16,777,215₁₀. The actual maximum, for the cell arrangement described in this report is 10,368,000 (= 12 x 864 x 1000). Keys less than 10,000,000 can be directly displayed using the EDIT processor (system). Otherwise the system processor, KFM (see Communications Research Centre User's (COMUS) Manual 5-2.13) must be invoked. Note that the keys as defined in FORTRAN are in the range [1,10368].

KEYKFM,F,K3.

This is used for accessing keys of ALLMON which are not compatible to EDIT. See also EXKEYKFM.

ACCMONB96,F,K3.

This is used for accessing cells from the unstandardized months, MONB96, upon specification of the cell indices. Statistics of the characteristics are also computed.

CELLCOUNT,F,K3.

This is for examining the quality of the cells of MONB96, as in Table 5.

CELLKEY,F,K3.

This is used for the construction of Table 6.

CHRZGRAD,F,K3.

This is applied to MONSTD in order to smooth foF2-Rz gradients. (See also Figures 6(a) and 6(b)).

Section 2.3

PREDSYS,F,K3.

This is the prediction program which uses keyed records of ALLMON to interpolate and predict ionospheric characteristics. It should be compiled with the BC option, as it contains the subroutines REGRESS, SLABTH, and DIVTEST. Also, to load, LYNX with BSSTEP1 and BSSTEP2.

REGRESS,F,K3.

This is used to prepare the arrays for the subroutines STEP1 and STEP2.

SLABTH,F,K3.

Slab thickness is computed for the user's input conditions, using the model illustrated in equation (3.18).

DIVTEST,F,K3.

Any positive integer is tested for divisibility by a given integer. This facilitates the accession of the 6 half months of data with 2 periods of local time each which are used in the model (2.13).

PRDATA,D,K3.

Each record contains a set of input conditions for making predictions at a given longitude, latitude, sunspot number, month, and magnetic activity. See also tape R033 for an example.

ADJRZ,D,C.

Preliminary interpolants (characteristics adjusted to the user's sunspot number) are displayed.

ADJKP,D,C.

The (at most) 12 triples of month and local time data are displayed.

REGFIT,D,C.

The details of the stepwise regression procedure for the model (2.13) are displayed.

SSTEP1 and SSTEP2,F,K3

These contain the subroutines STEP1 and STEP2 which perform the stepwise regression for fitting a characteristic as a function of local time and month.

NEWPLOT,F,K3

Contour maps of characteristics in local time and latitude are prepared. Compile with the BC option to include the subroutine CPLOTOPT.

CPLOTOPT,F,K3.

A modified version of the MLIB's contour plotting routine.

NEWPLOT1,D,C.

This contains the contour grids produced by PREDSYS. They may be (optionally) edited, using EDIT, before being input to NEWPLOT.

EXPREDSYS,X,K3.

This controls the entire procedure described in section 2.3.

Section 3.2.1

NHA,D,C.

A file consisting of original N(h) profiles in A Format (see Table 8).

NHB,D,C.

A file consisting of original N(h) profiles in B Format (see Table 8).

NHAMES,D,C.

A file consisting of original N(h) profiles in Ames Format (see Table 8).

KPFILE,D,C.

A file such that a record consists of the 8 3-hourly Kp indices together with the associated year and day.

NHXX,D,C.

A file consisting of reduced profiles in the format of ALOUETTE NH. XX are two integers denoting the satellite number in [1,2] and the volume number in [1,9] (see Table 8).

REDNHA,F,K3.

This produces a particular NHXX from a file NHA.

REDNHB,F,K3.

This produces a particular NHXX from a file NHB.

AMESPR,F,K3.

This produces a particular NHXX from a file NHAMES. It should be compiled with the "Batch Compile" (BC option) as it includes the subroutine FIELDAL.

NHCSB,D,C.

This consists of all the NHXX; concatenated, sorted (by universal time) and blocked (at the rate of 10 profiles per record). An extra byte (garbage) has been added to each profile to facilitate further buffering. The actual procedure is listed here in the execute file EXNHCSB.

```

EXNHCSB
!PCL DUMMY1
!SET F:SORTOUT/NHCSB;OUT
!SET F:SORTIN/NHC;IN
!SET M:SI/DUMMY2;IN
!SORT

```

where DUMMY1 consists of:

```

C NHXX,NHXX,...,NHXX INTO NHC
END

```

and DUMMY2 consists of:

```

.REC(103,104)
.KEYS(9,15)
.BLOCK(1, 10,DROP)

```

Section 3.2.2

THICKEX,F,K3.

Profiles from ALOUETTE NH are buffered in and a slab thickness is defined for each. These results are then sorted into cells, with an alignment specified by the user, and displayed in the form of a direct access file.

THICK,D,K11

The output of THICKEX.

THICKPR,F,K3.

THICK is read in a sequential fashion, and a model as in (3.18) is constructed. LYNX with BSSTEP1 and BSSTEP2.

Section 3.2.3

NHCS,D,C.

A selection of (unblocked) 103 byte profiles of ALOUETTE NH.

ALO,D,C.

A portion of a file ALOMONXX which contains the ionograms listed in NHCS.

ALOSNHMAT,F,K3.

A program which extends the records of NHCS (to 132 bytes) by attaching the foF2 and related parameters of ALOSYN. Table 9 was also produced by this program.

NHFOF2,D,C.

This is the output file produced by ALOSNHMAT.

GRECHO,D,C.

A file consisting of the output on unit 108 of RANDRUN.284201E (updated May 3, 1974 [J.H. Whitteker, private communications, 1978]). The card input (units 105 and 306) essentially consist of the scaled ground echoes (X wave) of the ionograms in NHFOF2. The Number density contour plots on unit 108 are not included.

GRECHOM,D,C.

A data file consisting of $m(n+1)$ records where m is the number of ionograms of NHFOF2 scaled for ground echoes and n is the number of pairs of echoes actually scaled for each ionogram. The extra record is an identification record (header) for each ionogram.

CGRECHO,F,K3.

The program which produces GRECHOM from the files NHFOF2 and GRECHO.

EAREC,F,K3.

The complete profiles, corresponding to those of NHCS, are input from NHA and NHB together with the file GRECHOM to compute a slab thickness. It should be compiled with the BC option (all non-standard subroutines are included). FIELDG of ORBIT.284201C and SOLVLE of .MLIB are required if a double precision version is desired. The input files GRECHOM, NHB, and NHA used for Table 12 are listed on tape 6E19, see below.

Section 4

TROCRT,F,K3.

A profile of a characteristic against latitude is created (as a smooth curve, using the subroutine CUBSPL, which is included) from a grid of the

characteristic, in the format of Table 6. Thus TROCRT should be compiled with the BC option. CUBSPL also uses SOLVLE which may be found in the source file SSOLVLE, for single precision use.

SSOLVLE,F,K3

A single precision version of the program SOLVLE, (in the library programs .MLIB of the Honeywell Sigma 9 computer) for solving a system of linear algebraic equations.

The actual tape serial numbers used in this report are now listed. Unless the contrary is stated these tapes are all 9 track, 800 bytes per inch, and free tapes. For labelled tapes, the serial number is the "internal" serial number, i.e. that written on the tape.

1. ALOSYN TAPES

(a) 6C47	September - December, 1962
(b) 6G03	January - April, 1963
(c) 4G48	May - December, 1963
(d) 4G49	January - December, 1964
(e) 4E26	January - December, 1965
(f) 1G47	January - December, 1966
(g) 1G48	January - December, 1967
(h) 1G49	January - December, 1968
(i) 3B02 or 6E21	MONB96, for all months.

2. ALOUETTE N(h) TAPES

(a) R541	Alouette 1, Volume 1
(b) R648	Alouette 1, Volume 2
(c) R034	Alouette 1, Volume 3
(d) R535	Alouette 1, Volume 4
(e) R568	Alouette 1, Volume 5
(f) R571	Alouette 1, Volume 6
(g) R033	Alouette 1, Volume 7, See 3(c), EXNHAL1.

(h) R037 Alouette 2, Volume 1
 (i) R752 Alouette 2, Volume 2
 (j) R582 Alouette 2, Volume 3
 (k) R740 Alouette 2, Volume 4
 (l) R570 Alouette 2, Volume 5
 (m) R022 Alouette 2, Ames 1
 (n) R720 Alouette 2, Ames 2
 (o) R739 Alouette 2, Ames 3
 (p) R749 Alouette 2, Ames 4
 (q) 5E46 or 3E30 ALOUETTE NH (or NHCSB)
 (r) 6E19 GRECHOM, (2427 records)
 NHB , (1201 records)
 NHA , (501 records)

3. MISCELLANEOUS TAPES

(a) 3B04 Kp , January 1962 - December 1970.
 (b) 5E47 *Labelled* tape (account 284201R, GLADWIN)
 This contains all the files which are available
 on request.
 (c) R033 *Labelled* tape (account 284201R, GLADWIN)
 This contains the data files
 ALLMON, CONTOUR, EXNHAL1, FOJAN63,
 FOFEB63, FOMAR63, PRDATA, THICK, ZR6278.
 (d) 5E08 Bottomside synoptics: January, 1969 - December, 1971
 (e) 4B32 Bottomside synoptics: January, 1972 - February, 1973
 (f) 4B33 Bottomside synoptics: January, 1973 - December, 1973
 (g) R603 Alouette 1 (103 byte) Profiles ; NHCS
 (h) R579 Alouette 1 (103 byte) Profiles ; NHCS
 (i) R565 Alouette 2 (103 byte) Profiles ; NHCS

APPENDIX B

List of Notations

1. Individual numbers are labelled by small English letters, possibly subscripted in the case of a serially related set of numbers.
2. File names (FORTRAN programs or data files) are labelled with capital letters.
3. The following notations are also used for denoting sets of numbers or files.
 - (a) $A = [a, b]$: The set of numbers lying between a and b including the end points, with the additional convention that a round bracket denotes exclusion of the end point, ($a < b$).
 - (b) $A = \{a, b, c, \dots\}$: The set of numbers consisting of $a, b, c \dots$.
 - (c) If the elements of A are serially related the following is used:

$$A = \{x_i : i = m(r)n\} = \{x_m, x_{m+r}, x_{m+2r} \dots, x_n\}$$
 - (d) The following are for combination of sets:

$A \cup B$: The set consisting of the elements in the set A or the set B .

$A \cap B$: The set consisting of the elements in the set A and the set B .

$A \times B$: The set of all combinations (pairs) of elements; the first from set A and the second from set B .

$A - B$: The set of elements in the set A but not in B .
4. Chapters, sections, and subsections are ordered lexicographically by a triple of integers. Equations are numbered consecutively within a given chapter, by a pair of numbers.

